

(1968).

<sup>33</sup>R. G. Gordon, *J. Chem. Phys.* **44**, 1830 (1966).<sup>34</sup>R. E. McClung, *J. Chem. Phys.* **51**, 3842 (1969).<sup>35</sup>G. D. Harp and B. J. Berne, *J. Chem. Phys.* **49**, 1249 (1968).<sup>36</sup>B. J. Berne, *J. Chem. Phys.* **56**, 2164 (1971).

PHYSICAL REVIEW A

VOLUME 7, NUMBER 3

MARCH 1973

## Multiple Exchange in the Quantum Crystals\*

A. K. McMahan<sup>†</sup> and R. A. Guyer*Department of Physics and Astronomy, University of Massachusetts, Amherst, Massachusetts 01002*

(Received 11 October 1972)

We develop the generalization of the Heisenberg near-neighbor-exchange Hamiltonian necessary to incorporate the effects of multiple-exchange processes. Many-body expressions for the multiple-exchange constants (pair exchange, triple exchange, and quadruple exchange) are derived. The physics that enters these exchange constants is discussed. For the most important of the pair and triple cases, these expressions are carefully evaluated using a Monte Carlo integration scheme. We show that the exchange Hamiltonian for solid <sup>3</sup>He is rapidly convergent, and that the near-neighbor pair, next-near-neighbor pair, and triple-exchange processes (involving two near neighbors and a next-near neighbor) are likely to be the only important exchange processes to the low-temperature thermodynamics of bcc <sup>3</sup>He. The magnitude of the triple-exchange process is such that the "effective" next-near-neighbor pair-exchange interaction in bcc <sup>3</sup>He is ferromagnetic. This result provides qualitative and quantitative support to the explanation of the data of Kirk and Adams made by Zane.

### I. INTRODUCTION

A quantum crystal is a crystal in which the zero-point displacement of a particle,  $\sqrt{\langle u^2 \rangle}$ , is a substantial fraction of the near-neighbor distance  $\Delta$ . Quite surprisingly, there are many macroscopic properties of the best-known quantum crystals (solid <sup>3</sup>He and solid <sup>4</sup>He) which appear relatively unaffected by this large zero-point motion. Simple thermostatic measurements, e. g., specific heat, thermal conductivity, etc., yield evidence for properties that are much like those of similar non-quantum crystals.<sup>1</sup> The truly unique experimental properties of the quantum crystals, however, are a consequence of the large zero-point motion, as manifested in the tunneling motions of the constituent particles. The wide variety of motionally narrowed nuclear magnetic resonance (NMR) phenomena in solid <sup>3</sup>He provide ample evidence for the presence of these tunneling motions.<sup>2</sup> The dominant motion that leads to this narrowing is the cooperative tunneling of a pair of near-neighbor <sup>3</sup>He atoms past one another, the exchange process. In crystals with vacancies, the tunneling of <sup>3</sup>He particles into vacant lattice sites leads to vacancy waves.<sup>3</sup> In crystals containing isotopic impurities the cooperative tunneling of an impurity atom and a neighboring host atom leads to "impuritons"<sup>4</sup> or "mass-fluctuation waves" (for dilute <sup>3</sup>He in <sup>4</sup>He).<sup>2,5</sup>

A discussion of the excitations that are a consequence of tunneling or a discussion of systems containing these excitations proceeds on two levels. *First* a qualitative description of the physics can

proceed from an assumed form for a model Hamiltonian or an assumed form for the dispersion relation. The work of Andreev and Lifshitz,<sup>4</sup> on "defectons" and "impuritons", Guyer and Zane<sup>5</sup> on "mass-fluctuation waves" and Guyer, Richardson, and Zane<sup>2</sup> in explanation of NMR phenomena are in terms of systems of excitations whose quantitative parameters are assumed known. For example, the behavior of solid <sup>3</sup>He at low temperatures is taken to be that of a near-neighbor Heisenberg antiferromagnet with the value of  $J$  being determined by experiment. *Second*, the model Hamiltonians employed in qualitative descriptions must be formally justified and a rigorous determination of the parameters that enter them must be implemented. These parameters depend strongly on the wave function of the system so that their determination constitutes an important test of the solution of the wave-function problem.

The near-neighbor pair-exchange Heisenberg Hamiltonian has in the past proved quite adequate in theoretical analyses of the thermodynamic<sup>6,7</sup> and NMR properties<sup>2,8</sup> of solid <sup>3</sup>He. An extensive literature<sup>9-17</sup> exists which reports calculations of the corresponding exchange parameter  $J$ , and adequate agreement with experiment has generally been obtained. We briefly review some of the recent progress reported in this literature later in this section. Recently, however, the excess pressure of solid <sup>3</sup>He in strong external magnetic fields has been measured by Kirk and Adams,<sup>18</sup> and found to be in disagreement with the predictions of the usual *near-neighbor pair-exchange* Heisen-

berg Hamiltonian. Zane<sup>19</sup> has suggested that this discrepancy is due to the significant presence of triple exchange in solid <sup>3</sup>He. He analyzed the experimental results in terms of an exchange Hamiltonian incorporating near- and next-near-neighbor pair-exchange processes and the most important triple-exchange process. He found the results of this analysis to be consistent with estimates of the size of the various exchange parameters involved, i. e., the Kirk and Adams experiment can be explained by assuming the presence of a triple-exchange process of reasonable magnitude.

The purpose of this paper is to present a thorough and rigorous treatment of a system in which pair and triple exchange occur. The exchange Hamiltonian used by Zane is formally justified, and calculations of exact expressions for the various frequencies involved are reported. An analysis of the relevant thermodynamics is given, with a view towards assessing which experimental measurements are best suited for detecting the presence of higher-order exchange processes in solid <sup>3</sup>He.

The organization and content of the paper is as follows: In Sec. II we exhibit the Hamiltonian describing the most important of the pair- and triple-exchange processes. It can be put in the form of a Heisenberg Hamiltonian with near-neighbor- and next-near-neighbor pair-exchange interactions, where the effect of the triple-exchange process has been to "renormalize" the two pair-exchange parameters (bcc structure). The most interesting aspect of this effect of triple exchange is that it may cause this renormalized next-near-neighbor pair-exchange interaction to be ferromagnetic. The thermodynamics of the Hamiltonian are presented in order to assess which physical properties are sensitive to the renormalized next-near-neighbor pair-exchange interaction. The experimental evidence is discussed in light of the possibility of discerning the presence of this process in the data. In Sec. III, the exchange Hamiltonian used to do the thermodynamics is formally justified. First-principles arguments are used to develop the exchange Hamiltonian containing all higher-order processes. General many-body expressions for the frequencies are given. In Sec. IV, these expressions are analyzed in detail to point out the effects which determine the size of the various exchange frequencies. It is shown that the only exchange processes which are likely to be important in solid <sup>3</sup>He are the near- and next-near-neighbor pair-exchange processes and the largest of the triple-exchange processes. Results of Monte Carlo calculations of the many-body surface integral expressions for these frequencies are presented. The Monte Carlo technique used is described in Appendix B. In Sec. V, we sum-

marize our findings and discuss the degree to which existing data or reasonable extensions of it can provide evidence for multiple-exchange processes. We conclude the present section with the discussion of the present status of the theory of near-neighbor exchange in solid <sup>3</sup>He. A number of details necessary to support the arguments presented in this discussion are given in Appendix A.

#### Near-Neighbor Pair-Exchange Problem

Since a substantial part of the new work reported in this paper will deal with numerical calculations of the parameters that characterize the pair- and triple-exchange processes it is appropriate for us to review the recent progress made in understanding the theory of calculations of this kind, and to make a statement about the justification for the particular computational procedure we employ.

The relevant literature begins with the calculation of Nosanow and Mullin<sup>9</sup> (see also Hetherington, Mullin, and Nosanow<sup>11</sup>). Nosanow and Mullin used a variational ansatz for the many-body wave function. At the level of the two-body cluster approximation, they calculated the expectation value of a pair Hamiltonian (which did not involve the lattice medium) with properly symmetrized two-body wave functions, and found  $J < 0$  and of approximately the correct order of magnitude. They also found the magnitude and sign of  $J$  to have a sensitive dependence on the detailed features of the wave function, particularly the short-range correlation function. Nosanow and Varma<sup>12</sup> extended this work to incorporate the phonons, and found substantially these same results. Subsequently, Guyer and Zane<sup>13</sup> (see also Guyer<sup>1</sup>) formulated the problem of pair exchange in terms of a two-body Hamiltonian which included an approximation to the lattice medium, and was thus used to shape the two-body wave function. Guyer and Zane cast the calculation of  $J$  in two forms: in terms of a surface integral that measured the probability current between configurations and in terms of a volume integral in which the contribution of various physical processes could be identified. They found, in agreement with Nosanow and Mullin, values of  $J$  less than zero and of approximately the right order of magnitude. In contrast to the work of Nosanow and Mullin, Guyer and Zane found the qualitative behavior of  $J$  to depend only upon the gross features of the wave function. Ebner and Sung<sup>14</sup> later presented a similar calculation, where the two-body Hamiltonian was obtained using a Green's-function technique. These theories, as well as the work of Thouless,<sup>10</sup> which did not present numerical results, have been critically reviewed by McMahan.<sup>17</sup> McMahan has also developed a rigorous theory for the calculation

of  $J$  based on an extension of the ideas of Herring<sup>20</sup> to the solid <sup>3</sup>He problem. This theory casts the calculation of  $J$  in the form of a many-body surface integral (see Thouless<sup>10</sup>). McMahan showed that the function to be used in the many-body surface integral was just the localized wave function, or home-base function, used in describing the lattice-dynamical behavior of the solid. Finally, McMahan calculated  $J$  using the many-body surface integral, a Monte Carlo integration scheme, and the home-base function generated by the ground-state calculations of Mullin and Nosanow. He found that many-body correlations—which are not included in any of the other present theories—suppress the calculated values of  $J$  at some densities by nearly an order of magnitude. Recently, as a part of an extensive field theoretic treatment of the quantum-crystal problem, Brandow<sup>15</sup> has cast the calculation of  $J$  in terms of a number of terms in perturbation theory. A few of these terms represent the contribution to  $J$  discussed by Guyer and Zane in their treatment of  $J$ . However, Brandow's very careful analysis has substantial differences in important details. Further Brandow finds additional contributions to  $J$  not discussed by Guyer and Zane that are important. Ostgaard<sup>16</sup> has implemented numerical calculations of the formulas due to Brandow. He also finds  $J < 0$  and of the correct order of magnitude. Further, Ostgaard finds sensitivity of sign and magnitude of  $J$  to essential features of the wave function. [Unfortunately, Ostgaard's results are questionable since the formulas owing to Brandow which he has evaluated contain a sign error; B. Brandow (private communication).]

At this point in our discussion, two concrete observations are possible. (i) All of the calculations of the magnitude of  $J$  in the literature, those of Nosanow and Mullin, Nosanow and Varma, Guyer and Zane, Ebner and Sung, and Ostgaard achieve fortuitous agreement with experiment. The effects of the many-body correlations neglected in these calculations are substantial. (ii) The use of the surface integral formulation of the calculation of  $J$  yields manifest antiferromagnetism ( $J < 0$ ) and insensitivity of the magnitude of  $J$  to all but the gross features of the wave function. This is in contrast to the results obtained using the perturbation-theory formulation. Is this owing to the inequivalence of these alternative formulations, the relative cumbersomeness of one compared to the other, or something else?

It is important to understand the relation of the surface integral formulation to the perturbation-theory results. Since the perturbation theories are based on an assumed two-body Schrödinger equation, or a closely related Bethe–Goldstone equation, we will consider the appropriate two-

body surface integral in making this comparison. In principle, the many-body short-range correlation effects mentioned in the first observation can be incorporated to some extent in such two-body formulations by taking more realistic choices for the single-particle potentials than the piecewise parabolic potentials that are usually taken. With this in mind, and also that we are now identifying  $J$  as half the singlet-triplet splitting of an appropriate two-body equation, our understanding of the situation is summarized here (these conclusions are justified in Appendix A):

(a) The surface integral formulation provides an exact expression for  $J$ .

(b) The numerical implementation of a calculation of  $J$  using this expression requires specification of the home-base functions.<sup>17,20</sup> Formally exact expressions for the home-base functions are possible in principle. Numerical calculations of  $J$  require the use of approximate home-base functions.

(c) The use of the surface integral expression with a given approximate home-base function gives the correct value of  $J$  to first order in the overlap integral  $p$ .<sup>13</sup> That is, corrections to  $J$  from further refinements of the home-base function are of order  $\hbar^2 J^2 / k_B \Theta_D$ . An equivalent statement is that the surface integral sums all first-order perturbation-theory contributions to  $J$ . As a consequence of this fact we may comment further about specific results for  $J$  that should be valid in general.

(d) The sign of  $J$  is negative and insensitive to the details of the home-base wave function, i. e., its quantitative features. If the usual form is taken, the sign of  $J$  is negative independent of both the Gaussian parameter  $A$  and the effective cutoff distance for the correlation function.

(e) The magnitude of  $J$  depends on the gross features of the home-base wave function in a simple and physically understandable way. See the discussion in Guyer and Zane,<sup>13</sup> McMahan,<sup>17</sup> and in Sec. IV of this paper.

(f) Aside from the basic necessity of its accounting for the hard cores of the atoms, the effects of the short-range correlation function are only to weakly modify the magnitude of  $J$ . Theories that show strong sensitivity of the sign and/or the magnitude of  $J$  to the short-range correlation function are inadequate.

(g) The magnitudes of  $J$  calculated using the presently available collection of home-base wave functions are generally far too small. A trivial repair of these wave functions in the tail, at  $|\vec{r}_1| \simeq \frac{1}{2} (\Delta^2 + \sigma^2)^{1/2} \simeq 0.6\Delta$ , will give excellent agreement with experiment. This repair is in the direction called for by physics and the calculations of Nosanow. The numerical determination of the

single-particle function by Nosanow<sup>21</sup> is very nearly Gaussian, but clearly exhibits a larger tail.

## II. THERMODYNAMICS WITH TRIPLE EXCHANGE

In this section we work out the thermodynamic properties of a spin- $\frac{1}{2}$  system in the presence of pair and triple exchange. Our purpose is to try and identify those properties of the system that are sensitive to higher-order exchange processes and to examine the large body of existing data to attempt to determine whether the presence of such processes has gone unnoticed in the data. The recent experiment of Kirk and Adams<sup>18</sup> is an exception in that it directly probes a quantity that is very sensitive to the triple-exchange process. We use the Kirk-Adams experiment to make an estimate of the rate of triple exchange. It is the estimate from this experiment against which we will test the theory of the magnitude of the triple-exchange process discussed in Sec. IV.

We begin by presenting the form of the exchange Hamiltonian with pair and triple exchange present. It is shown in Sec. III, that solid <sup>3</sup>He may be described by an effective Hamiltonian  $H_{\text{eff}}$ ,

$$\begin{aligned} H_{\text{eff}} &= H_L + H_X, \\ H_X &= -2 \sum_{i<j} \mathcal{J}_{ij} (\frac{1}{4} + \vec{I}_i \cdot \vec{I}_j) \\ &+ 2 \sum_{i<j<k} \mathcal{J}_{ijk} (\frac{1}{4} + \vec{I}_i \cdot \vec{I}_j + \vec{I}_j \cdot \vec{I}_k + \vec{I}_k \cdot \vec{I}_i) \\ &+ (\text{four-particle exchange}) + \dots, \end{aligned} \quad (1)$$

where  $\vec{I}_i$  is the nuclear spin operator for atom  $i$ . The motion of the atoms in the vicinity of their "own" lattice sites is described by the "lattice" Hamiltonian  $H_L$ . It thus describes the phononlike excitations of the solid. The more drastic motions of the atoms in which two or more switch places in the lattice is described by  $H_X$ , the exchange Hamiltonian. The first term in the exchange Hamiltonian describes pair exchanges, in which the pair of atoms  $i$  and  $j$  localized near the lattice sites  $\vec{R}_i$  and  $\vec{R}_j$ , respectively, make a transition to the arrangement in which they are localized near  $\vec{R}_j$  and  $\vec{R}_i$ , respectively. The second term describes triple exchanges in which the triple of atoms  $i$ ,  $j$ , and  $k$  localized near  $\vec{R}_i$ ,  $\vec{R}_j$ , and  $\vec{R}_k$ , respectively, make a transition to the arrangement in which they are localized near  $\vec{R}_j$ ,  $\vec{R}_k$ , and  $\vec{R}_i$ , respectively, or to the arrangement in which they are localized near  $\vec{R}_k$ ,  $\vec{R}_i$ , and  $\vec{R}_j$ , respectively.

The quantities  $\mathcal{J}_{ij}$  and  $\mathcal{J}_{ijk}$  appearing in Eq. (1) are exchange operators, which have matrix elements between the phononlike state of  $H_L$ . Their significance is simply that one must allow for the

possibility that the process of atoms exchanging places may be effected by the manner in which these same atoms are already moving according to their participation in whatever phonon state may happen to be excited in the system. In spite of this expectation, however, actual measurements on the exchange system in solid <sup>3</sup>He seem to be insensitive to any such operator nature of exchange. Analysis of the experimental results appears to be well handled by the approximation  $(\mathcal{J}_{ij})_{mn} \simeq J_{ij} \delta_{mn}$ . We shall, in fact, make this approximation in the discussion of this section, and take

$$\begin{aligned} H_X &= -2 \sum_{i<j} J_{ij} \vec{I}_i \cdot \vec{I}_j \\ &+ 2 \sum_{i<j<k} J_{ijk} (\vec{I}_i \cdot \vec{I}_j + \vec{I}_j \cdot \vec{I}_k + \vec{I}_k \cdot \vec{I}_i) \\ &+ (\text{four-particle exchange}) + \dots, \end{aligned} \quad (2)$$

where the uninteresting constant terms have been dropped. The relation of the exchange frequencies  $J_{ij}$  and  $J_{ijk}$  to the corresponding operators will be discussed later. We shall see in this section, as Zane<sup>19</sup> has pointed out, that the form of Eq. (2) is adequate to explain the Kirk and Adams results. Unfortunately, theoretical determination of the exchange frequencies are not sufficiently good to conclusively settle this matter. It should also be pointed out that Nosanow<sup>22</sup> has proposed an alternate interpretation of the Kirk-Adams results which depends crucially on the operator nature of exchange, namely that  $\langle \mathcal{J}_{ij}^2 \rangle$  is, in general, not equal to  $\langle \mathcal{J}_{ij} \rangle^2$ . The meaning of this statement is clear from an examination of Tables I, II, and III. To date, a calculation based on this approach has not been implemented.

We shall see in Sec. IV that the exchange frequencies drop off in size extremely rapidly as more atoms are involved, or as the atoms involved are more distant from each other. The notation used to refer to the various exchange processes and the corresponding frequencies is indicated in Fig. 1. The pair-exchange frequency  $J_{ij}$  is the same for all near- (next-near-) neighbor pairs  $i$  and  $j$ , and we designate this number by  $J_1$  ( $J_2$ ). The triple-exchange frequency  $J_{ijk}$  for any triplet  $i$ ,  $j$ , and  $k$ , in which the triangle contains two near-neighbor sides and one next-near-neighbor side is denoted by  $J_{112}$ , and so on. There is no (111) triangle in the bcc lattice. In Sec. IV it is seen that the only exchange processes in bcc <sup>3</sup>He which are likely to be important are the (1) and (2) pair, and the (112) triple processes. We shall retain only these in the exchange Hamiltonian given by Eq. (2). The pair contribution becomes

$$-2J_1 \sum_{i<j}^{(\text{nn})} \vec{I}_i \cdot \vec{I}_j - 2J_2 \sum_{i<j}^{(\text{nnn})} \vec{I}_i \cdot \vec{I}_j, \quad (3)$$

where nn and nnn signify that the sums are restricted to near-neighbor and next-near-neighbor pairs, respectively. Retaining only the (112) triple process, the triple-exchange Hamiltonian becomes

$$2J_{112} \sum_{\substack{i < j < k \\ (\text{restricted})}} (\vec{I}_i \cdot \vec{I}_j + \vec{I}_j \cdot \vec{I}_k + \vec{I}_k \cdot \vec{I}_i) \\ = 2J_{112} \left( 6 \sum_{i < j}^{(\text{nn})} \vec{I}_i \cdot \vec{I}_j + 4 \sum_{i < j}^{(\text{nnn})} \vec{I}_i \cdot \vec{I}_j \right), \quad (4)$$

where we have assumed a bcc geometry in arriving at this form. In terms of Eqs. (3) and (4), the exchange Hamiltonian is then

$$H_X = -2(J_1 - 6J_{112}) \sum_{i < j}^{(\text{nn})} \vec{I}_i \cdot \vec{I}_j - 2(J_2 - 4J_{112}) \sum_{i < j}^{(\text{nnn})} \vec{I}_i \cdot \vec{I}_j \\ + (\text{higher-order pair and triple}) \\ + (\text{four-particle exchange}) + \dots \quad (5)$$

We note that in the bcc phase, the primary effect of triple exchange is to "renormalize" both the near-neighbor pair-exchange parameter and the next-near-neighbor pair-exchange parameter. From Sec. IV we have  $|J_2| \approx |J_{112}| \ll |J_1|$  and  $J_1, J_2$ , and  $J_{112}$  all negative. Thus, in the case of the next-near-neighbor pair exchange, this renormalization

changes the sign of the exchange parameter. It is this effective *ferromagnetic* next-near-neighbor pair-exchange interaction in bcc  $^3\text{He}$  which appears to explain the results of Kirk and Adams, as will be discussed below.

We now treat the thermodynamics of the spin system in solid  $^3\text{He}$  taking the exchange Hamiltonian in the form

$$\mathcal{H}_X(V, H) = -2\Lambda_1(V) \sum_{i < j}^{(\text{nn})} \vec{I}_i \cdot \vec{I}_j - 2\Lambda_2(V) \sum_{i < j}^{(\text{nnn})} \vec{I}_i \cdot \vec{I}_j \\ - \gamma H \sum_i I_i^z, \quad (6)$$

where  $\Lambda_1(V) = (J_1 - 6J_{112})$ ,  $\Lambda_2(V) = (J_2 - 4J_{112})$ . We have added a Zeeman term  $\vec{\mu} \cdot \vec{H}$  for each spin and used the relation  $\vec{\mu} = \gamma \vec{I}$  ( $\gamma = 2.04 \times 10^4$  rad/G sec),  $\mu = \frac{1}{2} \gamma \hbar$ . In Eq. (6) we have explicitly displayed the volume dependence of  $J_1, J_2$ , and  $J_{112}$  in writing  $\Lambda_1(V)$  and  $\Lambda_2(V)$ . The magnetic pressure of the spin system is a consequence of the volume dependence of the spin energy manifested in  $\Lambda_1(V)$  and  $\Lambda_2(V)$ . The thermodynamic properties of the spin system follow from the equations

$$Z = \text{Tr} e^{-\beta \mathcal{H}_X}, \quad (7)$$

$$\beta F = -\ln Z, \quad (8)$$

$$P = -\left( \frac{\partial F}{\partial V} \right)_T, \quad (9)$$

$$S = -\left( \frac{\partial F}{\partial T} \right)_V, \quad (10)$$

$$\chi = -\frac{\partial^2 F}{\partial H^2}. \quad (11)$$

We will write out  $F, P, S$ , and  $\chi$  in the high-temperature limit.

The high-temperature limit is achieved by expanding  $e^{-\beta \mathcal{H}_X}$  in a power series in  $\beta \mathcal{H}_X$ . We have

$$\beta F = -N \ln 2 - \ln [1 + (\beta^2/2!) \langle \mathcal{H}_X^2 \rangle - (\beta^3/3!) \langle \mathcal{H}_X^3 \rangle + \dots], \quad (12)$$

where  $\langle A \rangle = \text{Tr}_s(A) / \text{Tr}_s(1)$  and  $\langle \mathcal{H}_X \rangle = 0$ . Thus, we have the power-series expansions of  $S, E, C, P$ , and  $\chi$  shown in Table I. The formulas in Table I exhibit the temperature dependence of each of these quantities as a power series in  $\beta$ . The coefficients of the various powers of  $\beta$  depend upon moments of the spin Hamiltonian or on  $V$  and  $H$  derivatives of these moments. We write  $\mathcal{H}_X$  in the form

$$\mathcal{H}_X = -2\Lambda_1(V) S_1 - 2\Lambda_2(V) S_2 - \gamma H S_3, \quad (13)$$

and obtain the values for  $\langle \mathcal{H}_X^2 \rangle, \langle \mathcal{H}_X^3 \rangle, \langle \mathcal{H}_X^2 \rangle_V, \langle \mathcal{H}_X^2 \rangle_{HH},$  and  $\langle \mathcal{H}_X^3 \rangle_{HH}$  shown in Table II. The quantities  $\gamma_1$  and  $\gamma_2$  (not to be confused with  $\gamma$  defined above) are the magnetic Grüneisen constants defined by

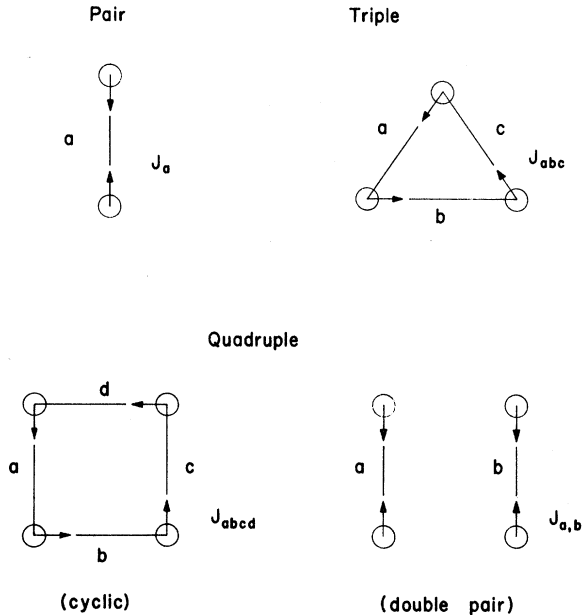


FIG. 1. Notation for the exchange constants. The various multiple exchange constants are labelled according to the sides of the figure traced out by the atoms in the course of their exchange. Thus  $J_1$  ( $J_2$ ) is the exchange constant for near-neighbor (next-near neighbor) pair exchange. Similarly, the triple-exchange frequency for a triangle containing two near-neighbor sides and one next-near-neighbor side is denoted by  $J_{112}$ .

TABLE I. Thermodynamic quantities. Power series in  $\beta$  for  $S, E, C, P$ , and  $\chi$ .

$$\begin{aligned} \frac{S(T, V, H)}{Nk_B} &= \ln 2 - \frac{1}{2}\beta^2 \langle \mathfrak{C}_x^2 \rangle + \frac{1}{8}\beta^3 \langle \mathfrak{C}_x^3 \rangle + O(\beta^4); \\ \frac{E(T, V, H)}{N} &= -\frac{1}{N} \frac{\partial \ln Z}{\partial \beta} = -\beta \langle \mathfrak{C}_x^2 \rangle + \frac{1}{2}\beta^2 \langle \mathfrak{C}_x^3 \rangle + O(\beta^3); \\ \frac{C(T, V, H)}{Nk_B} &= \frac{1}{Nk_B} \frac{\partial E}{\partial T} = \beta^2 \langle \mathfrak{C}_x^2 \rangle - \beta^3 \langle \mathfrak{C}_x^3 \rangle + O(\beta^4); \\ P(T, V, H) &= k_B T \frac{\partial \ln Z}{\partial V} = \frac{1}{2}N(\beta/V) [\langle \mathfrak{C}_x^2 \rangle_V - \frac{1}{8}\beta \langle \mathfrak{C}_x^3 \rangle_V + O(\beta^2)], \end{aligned}$$

where

$$\langle \dots \rangle_V = V \frac{\partial \langle \dots \rangle}{\partial V};$$

$$\chi(T, V, H) = \frac{k_B T}{N} \frac{\partial^2 \ln Z}{\partial H^2} = \frac{1}{2}\beta [\langle \mathfrak{C}_x^2 \rangle_{HH} - \frac{1}{8}\beta \langle \mathfrak{C}_x^3 \rangle_{HH} + O(\beta^3)],$$

where

$$\langle \dots \rangle_{HH} = \frac{\partial^2 \langle \dots \rangle}{\partial H^2}.$$

$$\gamma_1 = \frac{d \ln |\Lambda_1(V)|}{d \ln V}, \quad (14)$$

$$\gamma_2 = \frac{d \ln |\Lambda_2(V)|}{d \ln V}. \quad (15)$$

Combining the results in Tables I and II we have the power series in  $\beta$  and  $\mu H$  for  $S, E, C, P$ , and  $\chi$  displayed in Table III. We may examine these series to look for their sensitivity to the magnitude and sign of  $\Lambda_1$  and  $\Lambda_2$ .

It is apparent that the most direct handle on the presence of  $\Lambda_2$  is in the external field dependence of  $P(T, V, H)$ . In  $P(T, V, H)$  the quantity  $\beta(\gamma_1 \Lambda_1 + \frac{3}{4} \gamma_2 \Lambda_2)$  is the coefficient of the quadratic external field dependence; i. e.,

$$\begin{aligned} P(T, V, H) - P(T, V, 0) \\ = (N/V) 2(\gamma_1 \Lambda_1 + \frac{3}{4} \gamma_2 \Lambda_2) (\beta \mu H)^2 + \dots \quad (16) \end{aligned}$$

This quantity is sensitive to the *magnitude* and the *sign* of  $\Lambda_2$ . For the field-dependent excess entropy we have

TABLE II. Moments of  $\mathfrak{C}_x$ . These moments enter in the calculation of the thermodynamics [see Table I and Eq. (13)]. The spin sums required are  $\langle S_1^2 \rangle = \frac{3}{4}$ ,  $\langle S_2^2 \rangle = \frac{9}{16}$ ,  $\langle S_3^2 \rangle = \frac{1}{4}$ ,  $\langle S_1 S_2 \rangle = \frac{1}{2}$ ,  $\langle S_2 S_3 \rangle = \frac{3}{8}$ . We will drop terms proportional to  $\langle S_1^2 S_2 \rangle$ .

$$\begin{aligned} \langle \mathfrak{C}_x^2 \rangle &= 4\Lambda_1(V)^2 \langle S_1^2 \rangle + 4\Lambda_2(V)^2 \langle S_2^2 \rangle + \gamma^2 H^2 \langle S_3^2 \rangle, \\ \langle \mathfrak{C}_x^3 \rangle &= -24\Lambda_1(V)^2 \Lambda_2(V) \langle S_1^2 S_2 \rangle - 6\Lambda_1(V) \gamma^2 H^2 \langle S_1 S_3 \rangle - 6\Lambda_2(V) \gamma^2 H^2 \langle S_2 S_3 \rangle, \\ \langle \mathfrak{C}_x^2 \rangle_V &= 8\gamma_1 \Lambda_1(V)^2 \langle S_1^2 \rangle + 8\gamma_2 \Lambda_2(V)^2 \langle S_2^2 \rangle, \\ \langle \mathfrak{C}_x^3 \rangle_V &= -24(2\gamma_1 + \gamma_2) \Lambda_1(V)^2 \Lambda_2(V) \langle S_1^2 S_2 \rangle - 6\gamma_1 \Lambda_1(V) \gamma^2 H^2 \langle S_1 S_3 \rangle \\ &\quad - 6\gamma_2 \Lambda_2(V) \gamma^2 H^2 \langle S_2 S_3 \rangle, \\ \langle \mathfrak{C}_x^2 \rangle_{HH} &= 2\gamma^2 \langle S_3^2 \rangle, \\ \langle \mathfrak{C}_x^3 \rangle_{HH} &= -12\Lambda_1(V) \gamma^2 \langle S_1 S_3 \rangle - 12\Lambda_2(V) \gamma^2 \langle S_2 S_3 \rangle. \end{aligned}$$

TABLE III. Thermodynamic quantities as a function of  $\beta$  and  $\mu H$ .

$$\begin{aligned} S(T, V, H)/k_B N &= \ln 2 - \beta^2 [\frac{3}{8} \Lambda_1^2 + \frac{9}{8} \Lambda_2^2 + \frac{1}{2} (\mu H)^2] - \beta^3 [4\Lambda_1 (\mu H)^2 + 3\Lambda_2 (\mu H)^2] + \dots, \\ E(T, V, H)/N &= -\beta [3\Lambda_1^2 + \frac{9}{4} \Lambda_2^2 + (\mu H)^2] - \beta^2 [6\Lambda_1 (\mu H)^2 + \frac{9}{2} \Lambda_2 (\mu H)^2] + \dots, \\ C(T, V, H)/Nk_B &= \beta^2 [3\Lambda_1^2 + \frac{9}{4} \Lambda_2^2 + (\mu H)^2] + \beta^3 [12\Lambda_1 (\mu H)^2 + 9\Lambda_2 (\mu H)^2] + \dots, \\ P(T, V, H) &= (\beta/V) N \{ (3\gamma_1 \Lambda_1^2 + \frac{9}{4} \gamma_2 \Lambda_2^2) + \beta [2\gamma_1 \Lambda_1 (\mu H)^2 + \frac{3}{2} \gamma_2 \Lambda_2 (\mu H)^2] + \dots \}, \\ \chi(T, V, H) &= \beta \mu^2 [1 + \beta (4\Lambda_1 + 3\Lambda_2) + \dots]. \end{aligned}$$

$$S(T, V, H) - S(T, V, 0)$$

$$= -\frac{1}{2} (\beta \mu H)^2 [1 + 8\beta (\Lambda_1 + \frac{3}{4} \Lambda_2) + \dots] \quad (17)$$

The coefficient of the leading field dependence contains essentially the same dependence on  $\Lambda_1$  and  $\Lambda_2$  as the field-dependent excess pressure. But in this case the dependence on  $\Lambda_1$  and  $\Lambda_2$  appear relative to 1. Thus, the presence of  $\Lambda_2$  is less easily established by the analysis of entropy data (i. e., melting-curve data). These conclusions remain valid as the temperature is lowered toward  $T_N$ . Although, then, more terms in the high-temperature series must be retained.

There is no question that a relatively large value of  $\Lambda_2$  could be detected in field-independent experiments provided that  $\Lambda_1$  is known from independent sources sufficiently accurately or that two quantities sensitive to  $\Lambda_1$  and  $\Lambda_2$  in different ways could be measured with sufficient accuracy, e. g.,  $C(T, V, 0)$  and  $\chi(T, V, 0)$ . In view of the large body of data on all of the thermodynamic properties of  $^3\text{He}$  it is clear that the failure of the presence of  $\Lambda_2$  to have been noticed long ago is ample evidence for the inadequacy of quantitative tests for  $\Lambda_2$  in that data. This point is amplified in the following discussion.

How do you look for evidence of the presence of a new effect (a new term in the Hamiltonian)? If you expected the system to be described by a Hamiltonian like

$$\mathcal{H} = -2J \sum_{\langle i, j \rangle} \vec{I}_i \cdot \vec{I}_j \quad (18)$$

and you knew  $J$  very accurately, a single accurate measurement of one of  $S, E, \dots$  would tell you whether you have verified the theory of the behavior of the system given by Eq. (18) or not. If the theory were not verified by experiment (and the experiment not in doubt) you would expect to have to modify the Hamiltonian to include a new effect. If you expect the system to be described by Eq. (18) but you do not know  $J$  accurately, a test of the adequacy of Eq. (18) requires a measurement of two quantities that depend upon  $J$  in different ways. One of these measurements is used to determine  $J$ ; the second is used to verify Eq. (18). For example, in Table I we see that  $S,$

$E$ ,  $C$ , and  $P$  in zero external field all depend upon  $J$  in exactly the same way, i. e., through  $\langle \mathcal{H}_X^2 \rangle_{H=0}$ ,  $\langle \mathcal{H}_X^3 \rangle_{H=0}$ , etc. Thus measurements of  $S$ ,  $E$ ,  $C$ , and  $P$  are all equivalent and equally useful in determining  $J$ . At finite external field,  $J$  enters the determination of  $S$ ,  $E$ ,  $C$ , and  $P$  in a different way; different spin moments are involved (see Table II). Thus, the adequacy of Eq. (18) for describing the system can be tested by a measurement of one of  $S$ ,  $E$ ,  $C$ , and  $P$  at  $H=0$  and a measurement of one of  $S$ ,  $E$ ,  $C$ , and  $P$  at  $H \neq 0$ ; for example, a measurement of  $P(T, V, 0)$  to learn  $J$  and a measurement of  $P(T, V, H)$  to test the adequacy of Eq. (18) with this value of  $J$ . In the case we are dealing with here, the Heisenberg Hamiltonian required to describe solid  $^3\text{He}$ , we do not know the correct Hamiltonian and we do not know the magnitude of  $J$ . We must proceed to look at two essentially different measurements. It is clear that we do not have to look at most of the available data—for most of it is redundant in the sense described above and can tell us nothing new. The large body of NMR data on motionally narrowed phenomena is too complex in its interpretation to provide a reliable test. Experiments like the Kirk-Adams experiment or the high-field melting-curve experiments of Wheatley and co-workers<sup>23</sup> are potentially useful. The susceptibility data of the Brookhaven group<sup>24</sup> and the Cornell group<sup>25</sup> combined with the  $P(T, V, 0)$  data of Adams and co-workers is also potentially useful. However, a cursory glance at the uncertainties quoted in the susceptibility measurements of  $J$  make it clear that it will not be possible to use those data to verify the theory of  $\chi$  that would result from using Eq. (18) and  $J$  from Adams and co-workers (see Fig. 2). Thus, only the recent experiments by Kirk and Adams and Wheatley and co-workers can provide the required test. Of course, it was the Kirk-Adams experiment that motivated Zane's<sup>19</sup> suggestion about triple exchange.

It is clear from this discussion that an ideal experiment to look for the effects of  $\Lambda_2$  would be one at finite field that eliminates the trivial field dependence; e. g., the  $(\mu H)^2$  terms in  $S$  and  $C$ . For example experiments involving  $\partial/\partial V$  do this;

$$\frac{\partial M_x}{\partial V} = \frac{\partial P}{\partial H}.$$

To illustrate the power of the "right" experiment to see an effect, let us combine the prediction of Eq. (16) for the magnetic pressure in an external field with the data of Kirk and Adams. Kirk and Adams expected to see  $P(T, V, H)$  suppressed well below the value of  $P(T, V, 0)$  for suitably large external fields and low temperatures ( $H=60$  KG,  $T=30$  mK). The important point is that Kirk and Adams saw at most *half* of the change in  $P$  that they

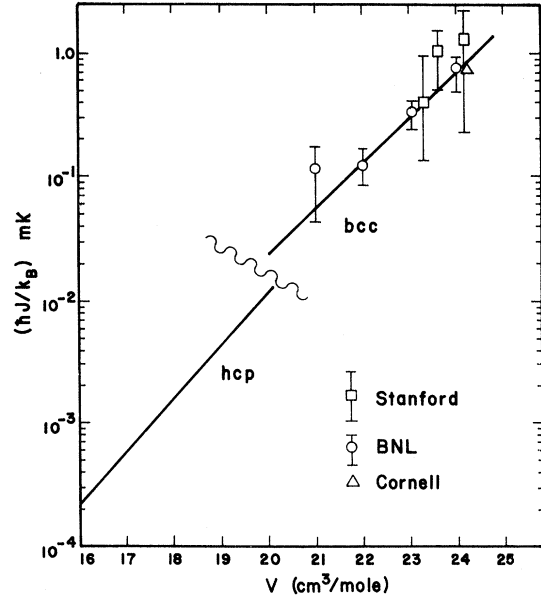


FIG. 2. Experimental information about  $J$ . A wide variety of NMR and thermodynamic data have been combined to yield the "best" value of  $J$  for each molar volume (the solid line). The direct measure of  $J$  from susceptibility data is shown with the error bars quoted in the experiments.

expected. Thus we argue from Eq. (16) that

$$\gamma_1 \Lambda_1 + \frac{3}{2} \gamma_2 \Lambda_2 \approx \frac{1}{2} \gamma_1 \Lambda_1. \quad (19)$$

This implies that  $\Lambda_2$  is opposite in sign from  $\Lambda_1$ , i. e., that the effective next-neighbor exchange interaction be ferromagnetic. For  $\gamma_1 \approx \gamma_2$ ,  $J_2 \approx J_{112}$ , and using the definitions of  $\Lambda_1$  and  $\Lambda_2$  below Eq. (6) we have [Essentially the same ratio is found ( $\frac{1}{18}$ ) if the results from Sec. IV are used, i. e., for a density  $V=24$  cm<sup>3</sup>/mole,  $\Delta=3.73$  Å, we find  $J_2 \approx 1.2 J_{112}$ ,  $\gamma_1 \approx 18$ , and  $\gamma_2 \approx 22$ .]

$$J_{112} \approx \frac{1}{15} J_1. \quad (20)$$

Thus, we see that a very small value of  $J_{112}$  will cause a substantial change in the thermodynamics and that  $P(T, V, H) - P(T, V, 0)$  is very sensitive to the presence of  $J_{112}$ .

### III. EXCHANGE HAMILTONIAN

In this section we generalize the discussion of the pair-exchange Hamiltonian for solid  $^3\text{He}$  presented elsewhere,<sup>17</sup> and develop an exchange Hamiltonian that includes higher-order exchange processes. Pair-, triple-, and quadruple-exchange processes are considered. Further, we derive the many-body volume, and where possible, the equivalent many-body surface integral expressions for the exchange frequencies that enter this Hamiltonian.

The exchange Hamiltonian is developed by a gen-

eralization of the well-known method of Dirac,<sup>26</sup> Heisenberg,<sup>27</sup> and Van Vleck.<sup>28</sup> The true Hamiltonian  $H$  acting on the space of properly antisymmetrized coordinate-spin functions is replaced by an effective Hamiltonian  $H_{\text{eff}}$  acting on a space of unsymmetrized coordinate-spin functions. The effective Hamiltonian is separable into two parts, one independent of spin and another dependent on spin,  $H_{\text{eff}} = H_L + H_X$ . The first part  $H_L$  describes the highly correlated motion of a fictitious system of distinguishable atoms moving in the vicinity of their "own" lattice sites. It is identified as the lattice Hamiltonian, and describes the phononlike excitations of the solid. The second spin-dependent part  $H_X$  describes the exchanges of these "distinguishable" atoms. It is identified as the exchange Hamiltonian. The coefficients of the spin operators in  $H_X$  are coordinate operators which may couple the states of  $H_L$ , and are taken to be the exchange operators. The necessity of exchange operators in the solid <sup>3</sup>He problem has been emphasized elsewhere.<sup>10,12</sup> Since the phononlike modes of  $H_L$  are more closely spaced in energy than the size of the exchange energy, the exchange process should be capable of creating and destroying phonons. This is the physical significance of the off-diagonal elements of these operators. The diagonal elements are essentially exchange frequencies corresponding to particular phonon states of the system. The physically meaningful exchange frequencies can be identified<sup>12</sup> with thermal averages of the exchange operators, using the density matrix for  $H_L$ .

We shall assume the true Hamiltonian of the system,  $H$ , to be spin independent. We are free to do this in solid <sup>3</sup>He since the contribution to the energy from the nuclear spin magnetic dipole-dipole interaction is more than three orders of magnitude smaller than that from near-neighbor pair exchange.<sup>29</sup> Our formal analysis of the higher-order exchanges will thus only be strictly correct for such processes which are also more important than this dipole-dipole interaction.

A crucial role is played in our development of the effective Hamiltonian by certain very special coordinate functions  $\{\phi_m\}$  called "home-base" functions by Herring.<sup>20</sup> A discussion of Herring's ideas as applied to solid <sup>3</sup>He appears elsewhere.<sup>17</sup> Two important properties of these functions are to be noted. (i) They are all localized in the same region of the configuration space of the  $N$  atoms in the sense that they are only large when, e.g., atom  $i$  is near lattice site  $i$ , for all  $i$ . (ii) The low-lying eigenstates of the system may be spanned by the set of states  $\{\alpha(\phi_m \xi_\alpha)\}$ , where  $\alpha$  is the antisymmetrizer and the  $\xi_\alpha$  are a complete set of orthonormal spin functions for the  $N$  atoms. The antisymmetrizer is given as usual in terms of

permutation operators

$$\alpha = (1/N!) \sum_P (-1)^P P, \quad (21)$$

where  $P = P^{(r)} P^{(s)}$ , and where  $P^{(r)}$  and  $P^{(s)}$  act on coordinate and spin variables, respectively. The second property allows one to find the low-lying physical eigenvalues of the system by diagonalizing  $H$  in the manifold  $\{\alpha(\phi_m \xi_\alpha)\}$ . The first property facilitates use of the expansion equation (21) since matrix elements  $\langle \phi_m | H P^{(r)} | \phi_n \rangle$  and  $\langle \phi_m | P^{(r)} | \phi_n \rangle$  become increasingly smaller as, according to  $P$ , the functions  $\phi_m$  and  $P^{(r)} \phi_n$  become farther separated from each other in configuration space. It has also been argued<sup>17</sup> that one may take the home-base functions such that

$$\langle \phi_m | H | \phi_n \rangle = E_n \delta_{mn}, \quad \langle \phi_m | \phi_n \rangle = \delta_{mn}, \quad (22)$$

which is equivalent, to lowest order, to their being the eigenfunctions of the lattice Hamiltonian  $H_L$ . Equation (22) does *not* imply that the  $\phi_m$  are eigenfunctions of  $H$ . By virtue of their being localized in the same region of configuration space, these functions do not form a complete set. The coordinate eigenfunctions of  $H$  are expected to be nonlocalized in that they must transform irreducibly under the permutation group. In fact, it is tempting to view the home-base functions as being the best-possible localized approximations to the true eigenfunctions of  $H$ .

We now develop the effective Hamiltonian in its most general form, using a straightforward extension of existing treatments for the problem of electronic exchange in insulators (see Herring's<sup>20</sup> review, especially pp. 128–135). The physical eigenvalues are given by

$$\det(\langle \phi_m \xi_\alpha | H \alpha | \phi_n \xi_\beta \rangle - E \langle \phi_m \xi_\alpha | \alpha | \phi_n \xi_\beta \rangle) = 0. \quad (23)$$

These same eigenvalues may be generated by  $H_{\text{eff}}$  acting on the unsymmetrized space  $\{\phi_m \xi_\alpha\}$ , i.e.,

$$\det(\langle \phi_m \xi_\alpha | H_{\text{eff}} | \phi_n \xi_\beta \rangle - E \delta_{mn} \delta_{\alpha\beta}) = 0, \quad (24)$$

if one defines

$$\langle \phi_m \xi_\alpha | H_{\text{eff}} | \phi_n \xi_\beta \rangle = N! \sum_{\substack{m' \alpha' \\ n' \beta'}} (D^{-1/2})_{m\alpha, m'\alpha'} \\ \times \langle \phi_{m'} \xi_{\alpha'} | H \alpha | \phi_{n'} \xi_{\beta'} \rangle (D^{-1/2})_{n'\beta', n\beta}, \quad (25)$$

where

$$(D^{-1/2})_{m\alpha, n\beta} = \delta_{mn} \delta_{\alpha\beta} - \frac{1}{2} \Delta_{m\alpha, n\beta} + \frac{3}{8} (\Delta^2)_{m\alpha, n\beta} - \dots, \quad (26)$$

$$D_{m\alpha, n\beta} \equiv N! \langle \phi_m \xi_\alpha | \alpha | \phi_n \xi_\beta \rangle = \delta_{mn} \delta_{\alpha\beta} + \Delta_{m\alpha, n\beta}, \quad (27)$$

$$\Delta_{m\alpha, n\beta} = \sum_P (-1)^P \langle \phi_m \xi_\alpha | P | \phi_n \xi_\beta \rangle. \quad (28)$$

The prime in Eq. (28) signifies that  $P$  cannot be the identity permutation  $E$ . Since the spin sums run over a complete set of spin states, Eq. (25) may be put in the form



$$H_{\text{eff}} = H_L + \sum'_P (-1)^P \mathcal{J}_P P^{(\sigma)} , \quad (29)$$

where  $H_L$  and  $\mathcal{J}_P$  are coordinate operators given, in general, by

$$\langle \phi_m | \mathcal{J}_P | \phi_n \rangle = \sum_{Q,R} \sum_{m',n'} (G^{-1/2})_{Em, Qm'} \times \langle \phi_{m'} | HQ^{(r)-1} P^{(r)} R^{(r)} | \phi_{n'} \rangle (G^{-1/2})_{Rn', En} , \quad (30)$$

$$(G^{-1/2})_{Qm, Rn} = \delta_{QR} \delta_{mn} - \frac{1}{2} \Omega_{Qm, Rn} + \frac{3}{8} (\Omega^2)_{Qm, Rn} - \dots , \quad (31)$$

$$G_{Qm, Rn} \equiv \langle \phi_m | Q^{(r)-1} R^{(r)} | \phi_n \rangle = \delta_{QR} \delta_{mn} + \Omega_{Qm, Rn} . \quad (32)$$

(Note that  $G_{PQm, PRn}$  is independent of  $P$ , and that  $G^{-1/2}$  has the same property.)  $H_L$  is given by Eq. (30) with  $P=E$ . Expanding Eq. (30), the first few terms for  $\mathcal{J}_P$  may be written

$$\begin{aligned} \langle \phi_m | \mathcal{J}_P | \phi_n \rangle &= \langle \phi_m | (H - \frac{1}{2} E_m - \frac{1}{2} E_n) P | \phi_n \rangle \\ &- \frac{1}{2} \sum'_Q \sum_i \langle \phi_m | Q^{-1} | \phi_i \rangle \langle \phi_i | (H - \frac{1}{2} E_m - \frac{1}{2} E_n) Q P | \phi_n \rangle \\ &+ \langle \phi_m | (H - \frac{1}{2} E_m - \frac{1}{2} E_n) P Q | \phi_i \rangle \langle \phi_i | Q^{-1} | \phi_n \rangle + \dots . \end{aligned} \quad (33)$$

We have omitted the superscript “ $r$ ” on these permutations, and will do so henceforth when unambiguous. The dominant contribution to  $\langle \phi_m | H_L | \phi_n \rangle$  is  $E_n \delta_{mn}$ , with second-order corrections given by Eq. (33) with  $P=E$ . We have added and subtracted  $\frac{1}{2} [\delta_{PE} \delta_{mn} (E_m + E_n)]$  in Eq. (30) to arrive at Eq. (33). This constitutes a very helpful partial summation of the whole series in Eq. (30) as can be seen by the fact that without this alteration, the second-order term in Eq. (33) would have contained a first-order contribution when  $Q=P^{-1}$ .

The  $\mathcal{J}_P$  are the exchange operators, corresponding to the particular exchange processes indicated by the permutations  $P$ . The increasing number of multiple sums over all permutations occurring in the definition is a manifestation of the well-known nonorthogonality catastrophe.<sup>30</sup> Intuitively, one expects this expansion in powers of the overlap to be valid, and that all terms exhibiting unphysical dependence on  $N$  to cancel out. Although no general proof for our case exists, such cancellation has been proved for special cases,<sup>30</sup> which strengthens this intuitive feeling. For example, if only a single coordinate state  $\phi_0 = \prod_i \phi_i(i)$  were used in the derivation, terms involving  $\langle \phi_0 | (H - E_0) Q P | \phi_0 \rangle$  in one order would be largely cancelled by terms involving  $-\langle \phi_0 | Q | \phi_0 \rangle \langle \phi_0 | (H - E_0) P | \phi_0 \rangle - \langle \phi_0 | P | \phi_0 \rangle \langle \phi_0 | (H - E_0) Q | \phi_0 \rangle$  in the next. Only  $Q$ 's which permute groups of atoms such that at least one is relatively close, with respect to the range of the two-body potential, to an atom permuted by  $P$  would contribute. These same comments apply if  $P$  itself is factorable, e.g., a double-pair exchange  $P = P_{ij} P_{kl}$ , and so one expects  $\mathcal{J}_{ij, kl} \rightarrow 0$  as the pairs  $(i, j)$  and  $(k, l)$  move apart. One believes

it is these restrictions which leave the expansions for  $\mathcal{J}_P$  of order unity and that for  $H_{\text{eff}}$  of order  $N$ .

Assuming we are not troubled by problems of the dependence on  $N$ , it still remains to decide whether the higher-order terms in Eq. (33) are important. One might crudely describe their significance in the language of Thouless's<sup>10</sup>  $N!$  cavities. The system is initially in the state  $\phi$ , according to which it is predominantly found in the cavity we shall label by the identity permutation  $E$ . The first term in Eq. (33) corresponds to its evolving directly from this cavity to the exchanged cavity  $P$ . Since the state  $\phi$  is not orthogonal to its permuted counterparts, there is also a small probability that the system may momentarily occupy some state  $Q^{-1}\phi$ , which is large not in the cavity  $E$ , but instead, in some nearby cavity  $Q^{-1}$ . Contributions to the second term in Eq. (33) can then be loosely associated with the system evolving from the original to the exchanged cavity by an indirect route, in which it passes through some intermediate cavity along the way. It is plausible to expect the relative importance of these two terms to be given by

$$\langle \phi | P \phi \rangle \quad (34a)$$

and

$$\sum'_Q \langle \phi | Q^{-1} \phi \rangle \langle Q^{-1} \phi | P \phi \rangle , \quad (34b)$$

respectively, where the sum in Eq. (34b) is over cavities which are near to those designated by  $E$  and  $P$ . As a first approximation, we might use

$$\phi = C \prod_i e^{-A(\vec{r}_i - \vec{R}_i)^2/2} ,$$

where  $\vec{r}_i$  and  $\vec{R}_i$  are the atom and lattice position vectors, respectively. The matrix element  $\langle \phi | P | \phi \rangle$  is then  $e^{-Ad^2/4}$ , where  $d$  is the distance in configuration space between the representative points corresponding to the  $E$  and  $P$  equilibrium arrangements of the atoms on the lattice sites. We shall see in more detail later that  $e^{-Ad^2/4}$  drops off extremely rapidly as the permutation  $P$  involves larger numbers of atoms, or as the atoms involved are farther separated from each other in the lattice. Let us consider the (1) pair case, i.e.,  $P$  is a first-neighbor pair permutation. The largest contributions to Eq. (34b) will come from  $Q^{-1}$  and  $QP$  being (1) pair and (112) triple permutations, respectively, and vice versa. An examination of the geometry shows there to be six possibilities for each of these choices. Taking  $A = 1.30 \text{ \AA}^{-2}$  and a density corresponding to a near-neighbor distance  $\Delta = 3.75 \text{ \AA}$ , the quantity  $e^{-Ad^2/4}$  is  $2.4 \times 10^{-7}$  for the (112) permutation. Thus the leading contributions to Eq. (34b) yield a value for this expression a factor of about  $3 \times 10^{-6}$  times smaller than Eq. (34a). This strongly suggests that for

the (1) pair-exchange operators, the second- and higher-order terms in Eq. (33) are completely negligible. The same kind of analysis suggests that any of the processes for which the quantity  $e^{-Ad^2/4}$  is relatively large, are well represented by the first term in Eq. (33). In particular, we mention the (1) and (2) pair, the (112) triple, and the (1111) quadruple processes. If one considers the effect of the hard-core repulsion between  ${}^3\text{He}$  atoms, the pair-permutation overlap will be severely reduced; the triple and cyclic four-particle overlap, much less so. This further reduces the effect of the higher-order terms in Eq. (33) for the processes we have listed above. It also suggests that the dominant four-particle processes are the cyclic ones.

For what processes will the higher-order terms in Eq. (33) be important? Following the intuitive ideas just mentioned, one would expect these terms to be important if there exists an indirect route between the original and exchanged cavities which is nearly as important, or more important, than the direct route. More precisely, they should be important if there exists a cavity  $Q$  such that  $d_{EQ}^2 + d_{QP}^2 \lesssim d_{EP}^2$ , where  $d_{EQ}$  is the distance between the cavities labeled  $E$  and  $Q$ . A typical example for which this is the case is a triple exchange in which the triangle has an angle near, or greater than  $90^\circ$ . Although it should be mentioned, that the indirect route in this case involves a pair overlap which will be considerably reduced in size relative to the triple overlap due to the hard-core interactions. This will tend to decrease the importance of the higher-order terms here. Finally, in the case of any exchange described by a factorable permutation, such as the four-particle double exchange  $P_{ij}P_{kl}$ , certain of the "second-order" terms are identical in size to the first terms, as is clearly necessary in order to have the cancellation which one expects to cause  $\mathcal{J}_{ij,kl}$  to vanish if the pairs are too distant.

The spin permutation operators appearing in Eq. (29) may be expressed in terms of the nuclear spin operators  $I_i$  by using

$$P_{ij}^{(\sigma)} = \frac{1}{2} + 2\vec{I}_i \cdot \vec{I}_j \quad (35)$$

and building up the more complex permutations from this. One uses

$$(\vec{I}_i \cdot \vec{I}_j)(\vec{I}_i \cdot \vec{I}_k) = \frac{1}{4}\vec{I}_i \cdot \vec{I}_k + \frac{1}{2}\vec{I}_i \cdot \vec{I}_j \times \vec{I}_k \quad (36)$$

to reduce terms containing more than one spin operator for the same atom. Having done so, one sees that  $P^{(\sigma)} + P^{(\sigma)-1}$  and  $P^{(\sigma)} - P^{(\sigma)-1}$  contain only terms with an even number and odd number, respectively, of the spin operators. The usual argument (Ref. 20, p. 23) of Hermiticity and time-reversal symmetry does not suffice in our case to eliminate the terms with an odd number of spin

operators since their coefficients are now (coordinate) operators. However, it does imply that these operators must be antisymmetric, and thus can only contribute to the energy in second-order perturbation theory. We shall consequently neglect them. The remaining terms in Eq. (29) are of the form  $\frac{1}{2}(\mathcal{J}_P + \mathcal{J}_{P^{-1}})(P^{(\sigma)} + P^{(\sigma)-1})$ . Since  $\mathcal{J}_{P^{-1}} = \mathcal{J}_P^\dagger$ , this leads to a sensible redefinition of the exchange operators as  $\frac{1}{2}(\mathcal{J}_P + \mathcal{J}_P^\dagger)$ , so that they will be Hermitian.

We now exhibit the exchange Hamiltonians for pair, triple, and cyclic four-particle exchange.

$$H_X^{(2)} = -2 \sum_{i < j} \mathcal{J}_{ij} \left( \frac{1}{4} + \vec{I}_i \cdot \vec{I}_j \right), \quad (37)$$

$$H_X^{(3)} = 2 \sum_{i < j < k} \mathcal{J}_{ijk} \left( \frac{1}{4} + \vec{I}_i \cdot \vec{I}_j + \vec{I}_j \cdot \vec{I}_k + \vec{I}_i \cdot \vec{I}_k \right), \quad (38)$$

$$H_X^{(4c)} = - \sum_{i < j < k < l} (\mathcal{J}_{ijkl} \mathcal{S}_{ijkl} + \mathcal{J}_{ijlk} \mathcal{S}_{ijlk} + \mathcal{J}_{ikjl} \mathcal{S}_{ikjl}), \quad (39)$$

where

$$\begin{aligned} \mathcal{S}_{ijkl} = & \frac{1}{4} + \vec{I}_i \cdot \vec{I}_j + \vec{I}_i \cdot \vec{I}_k + \vec{I}_i \cdot \vec{I}_l + \vec{I}_j \cdot \vec{I}_k + \vec{I}_j \cdot \vec{I}_l + \vec{I}_k \cdot \vec{I}_l \\ & - 4\vec{I}_i \cdot \vec{I}_k \vec{I}_j \cdot \vec{I}_l + 4\vec{I}_i \cdot \vec{I}_j \vec{I}_k \cdot \vec{I}_l + 4\vec{I}_i \cdot \vec{I}_j \vec{I}_k \cdot \vec{I}_l. \end{aligned}$$

The (Hermitian) exchange operators are given by

$$\langle \phi_m | \mathcal{J}_P | \phi_n \rangle = \langle \phi_m | (H - \frac{1}{2}E_m - \frac{1}{2}E_n)^{\frac{1}{2}} (P + P^{-1}) | \phi_n \rangle, \quad (40)$$

where this approximation should be valid for the few largest of each of the pair, triple, and cyclic four-particle processes. Extending an identification made<sup>12</sup> for pair exchange, we take the exchange frequencies

$$J_P = \text{Tr}(\rho_L \mathcal{J}_P), \quad (41)$$

where  $\rho_L$  is the density matrix for the lattice Hamiltonian  $H_L$ . In calculations of  $J_P$  for near-neighbor pair exchange, it has been found,<sup>12</sup> at the low temperatures for which solid  ${}^3\text{He}$  exists, that the temperature dependence of Eq. (41) is negligible. It is thus plausible to approximate Eq. (41) in general by its  $T=0$  value,

$$J_P \simeq \langle \phi_0 | \mathcal{J}_P | \phi_0 \rangle \quad (42)$$

$$= \text{Re} \langle \phi_0 | (H - E_0) P | \phi_0 \rangle, \quad (43)$$

where by taking the real part of the matrix element in Eq. (43) we may eliminate the reverse permutation.

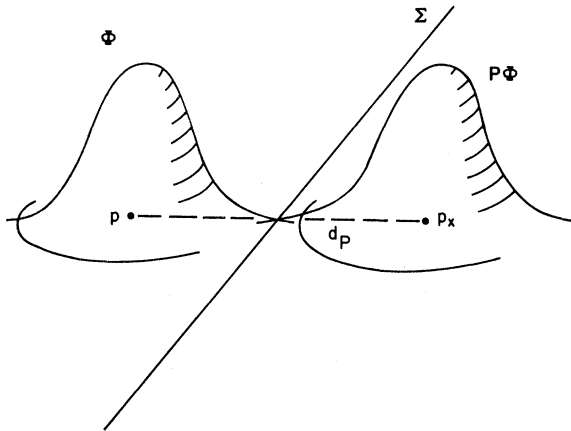
In previous work,<sup>10,17</sup> a method due to Herring<sup>20</sup> has been used to represent the matrix elements of  $\mathcal{J}_{ij}$  in terms of many-body hypersurface integrals. Herring's method is based on the assumption that the home-base functions may be approximated by the eigenfunctions of a certain truncated Hamiltonian. While the surface integral may be derived in a more rigorous fashion, we shall briefly review this more intuitively appealing method here for the general case of Eq. (43). We

then indicate the more rigorous approach, and point out certain cases where Eq. (43) cannot be represented by an equivalent surface integral.

The truncated Hamiltonian  $H_T$  is obtained from the true Hamiltonian  $H$  by eliminating the attractive parts of all but one of the  $N!$  permutationally equivalent local potential wells of its many-body potential. These local wells correspond to the various equilibrium arrangements of the  $N$  atoms on the  $N$  lattice sites. The eigenfunctions of the truncated Hamiltonian will thus be localized, in the configuration space of the  $N$  atoms, about the one remaining well. One assumes that these eigenfunctions and the corresponding eigenvalues are reasonable approximations to the home-base functions  $\phi_m$  and energies  $\langle \phi_m | H | \phi_m \rangle = E_m$ . Since  $H_T$  differs from  $H$  only in the vicinity of the other  $N! - 1$  wells, one may then assume that  $(H - E_m)\phi_m = 0$  except near these other wells.

Given Eq. (43), let  $\Sigma$  be the hypersurface in configuration space separating, and midway between, the regions where  $\phi_0$  and  $P\phi_0$  are large, the former being on the "near" side; the latter, the "far" side (see Fig. 3). If there are no other local wells of the full potential, except the two under consideration, in the vicinity of the region where  $\phi_0^* P\phi_0$  is large, we may take for use in Eq. (43):

$$(H - E_0)\phi_0 = 0 \text{ near side of } \Sigma ,$$



Configuration Space of the  $N$  Atoms

FIG. 3. Schematic representation of the configuration space of  $N$  atoms. The home-base function  $\phi$  is localized about the  $3N$ -dimensional point  $p$ , which corresponds to some given arrangement of the atoms on the lattice sites. The function  $P\phi$  is obtained from  $\phi$  by interchanging a number of atoms according to the permutation  $P$ , and is localized about the exchanged point  $p_x$ . The number  $d_p$  is the distance between  $p$  and  $p_x$ , and  $\Sigma$  is a  $(3N-1)$ -dimensional hypersurface which bisects and is perpendicular to the line between these two points. The exchange constant  $J_p$  is a measure of the frequency with which the system evolves from the state  $\phi$  to the state  $P\phi$  and back again.

$$(H - E_0)P\phi_0 = 0 \text{ far side of } \Sigma . \quad (44)$$

Combining Eqs. (43) and (44) and integrating by parts one gets

$$J_p = -\frac{\hbar^2}{2m} \text{Re} \int_{\Sigma} d\vec{S} \cdot [\phi_0^* \nabla_{3N} P\phi_0 - (P\phi_0) \nabla_{3N} \phi_0^*] , \quad (45)$$

where  $d\vec{S}$  is the  $(3N-1)$ -dimensional surface element whose direction is perpendicular to  $\Sigma$  and from the "near" to the "far" side and  $\nabla_{3N}$  is the  $3N$ -dimensional gradient.

The crucial issue is of course the validity of Eq. (44). To gain some insight, we turn to the more formal derivation. An essential feature in the definition<sup>17,20</sup> of the home-base functions was that the set  $\{P\phi_m\}$  exactly spans a particular set of the coordinate eigenfunctions of  $H$ . (These are coordinate permutations.) This implies

$$H\phi_m = \sum_{Q,n} (C_Q)_{mn} Q^{-1} \phi_n , \quad (46)$$

where by using Eqs. (31) and (32) one can see that the  $(C_Q)_{mn}$  are closely related to  $(\mathcal{G}_Q)_{mn}$  given by Eq. (33). In fact, to lowest order

$$(C_E)_{mn} \simeq (H_L)_{mn} \simeq E_m \delta_{mn} ,$$

$$(C_Q)_{mn} \simeq (\mathcal{G}_Q)_{mn} \simeq \langle \phi_m | (H - \frac{1}{2} E_m - \frac{1}{2} E_n) Q | \phi_n \rangle .$$

The virtue of Eq. (46) is that it allows one to actually determine the expressions  $(H - E_0)\phi_0$  and  $(H - E_0)P\phi_0$  in terms of the constants  $(C_Q)_{mn}$  and the various states  $Q^{-1}\phi_n$ . One can immediately see that the error made by using Eq. (44) in Eq. (43) is essentially of the form of the second- and higher-order terms in Eq. (33). The numerical coefficients are slightly different, and some of the overlap matrix elements are only integrated over the "near" or "far" half-space. The essential point, however, is that the same arguments used previously to judge the importance of these terms apply here. Two conclusions are evident: (i) It is precisely when the lowest-order approximation, Eq. (40), for the exchange operator is valid, that one may also obtain the surface integral. In particular, Eq. (45) is equivalent to Eq. (43) for the (1) and (2) pair, the (112) triple, and the (1111) four-particle exchange frequencies. (ii) The surface integral does follow directly from the volume integral using the properties of the true home-base functions, and without resorting to the idea of the truncated Hamiltonian approximation to the home-base functions.

#### IV. FREQUENCIES

In this section we investigate the various effects which determine the size of the  $T=0$  exchange frequencies. The analysis is based on the many-body surface integral expression given by Eq. (45), taking the Nosanow-Mullin<sup>9</sup> approximation to

the home-base function. It is seen that the exchange Hamiltonian for solid  $^3\text{He}$  is rapidly convergent, and that the only important exchange processes are the (1) and (2) pair and the (112) triple processes. Certain inadequacies in Zane's<sup>19</sup> estimates of the size of these frequencies are pointed out. We report extensive Monte Carlo evaluations of the full many-body surface integral expressions for these frequencies. It is seen that the (112) triple frequency is approximately equal to the (2) pair frequency except at the higher densities, where it is somewhat larger. Thus the effective second-neighbor exchange interaction in bcc  $^3\text{He}$  is ferromagnetic, as Zane has suggested. A conclusive determination of the ratio  $J_{112}/J_1$  is hindered by the uncertainty as to what Gaussian parameters and correlation functions should be used, as well as the possibility that the tail of a Gaussian single-particle function may be inadequate for exchange calculations. We conclude with a brief discussion of these difficulties, which are common to all existing exchange calculations in solid  $^3\text{He}$ .

We suggested earlier that the many-body surface integral, Eq. (45), gives the first- and second-neighbor pair and the largest triple-exchange frequencies exactly to leading order if the true home-base function  $\phi_0$  is used or, one may reasonably expect, if  $\phi_0$  is approximated by the ground-state eigenfunction of the truncated Hamiltonian. The latter function may be approximated variationally by minimizing the energy, subject to the constraint that the variational ansatz be localized. This is precisely what Nosanow *et al.*,<sup>21,11</sup> Hansen and Levesque,<sup>31</sup> and others have done, taking the ansatz

$$\phi = C \prod_i e^{-A(\vec{r}_i - \vec{R}_i)^2/2F}, \quad F = \prod_{i < j} f(r_{ij}), \quad (47)$$

where  $\vec{r}_i$  and  $\vec{R}_i$  are the atom and lattice-site position vectors, respectively, and  $f(r_{ij})$  are the short-range correlation functions. In any such practical calculation, the extent to which  $\phi$  approximates  $\phi_0$  is not at all clear. However, functions of the form given by Eq. (47) have proved quite successful in calculations of the ground-state energy, and give order-of-magnitude agreement with experiment for first-neighbor pair exchange. Whether they are adequate to give closer agreement in exchange calculations cannot be settled until the choice of  $A$  values and correlation functions can be agreed upon. The physical significance of the factors in Eq. (47) is clear. The Gaussian part describes the atoms vibrating about their lattice sites, and constitutes an Einstein approximation to the more general correlated Gaussian which would describe the phonons.

The short-range correlations serve to cut the

wave function off when any two atoms get closer than their hard-core radius, a feature necessitated by the large zero-point motion in solid  $^3\text{He}$ . We shall base our discussion of the exchange frequencies on the use of Eq. (47) in Eq. (45), and take the Nosanow correlation function

$$f(r) = e^{-K[(\sigma/r)^{12} - (\sigma/r)^6]}, \quad (48)$$

$$\sigma = 2.556 \text{ \AA}, \quad K = 0.1778$$

in numerical computations. We expect the effect of the phonons on the first-neighbor pair frequency to be of somewhat lesser importance than those we will be describing, as will be pointed out at the end of this section. However, it is conceivable that the phonons might lead to interesting directional effects in some of the higher-order processes which our discussion will not include. The effects of other correlation functions will be mentioned.

The general expression for the exchange frequencies using the approximation Eq. (47) for  $\phi_0$  in Eq. (45) may be found after some manipulation to be

$$J_P = - \frac{\hbar^2 A d_P}{2m} \frac{\int d\tau \delta(u_1) \phi P \phi}{\int d\tau \phi^2}, \quad (49)$$

where  $d\tau = d\vec{r}_1 \dots d\vec{r}_N$ , and where

$$u_1 = \hat{n} \cdot (\vec{r}_1, \vec{r}_2, \vec{r}_3, \dots, \vec{r}_N),$$

$$\hat{n} = \frac{1}{d_P} (p_x - p),$$

$$p = (\vec{R}_1, \vec{R}_2, \vec{R}_3, \dots, \vec{R}_N), \quad (50)$$

$$p_x = (P\vec{R}_1, P\vec{R}_2, P\vec{R}_3, \dots, P\vec{R}_N),$$

$$d_P = \|p_x - p\| = \left( \sum_i (P\vec{R}_i - \vec{R}_i)^2 \right)^{1/2}.$$

We have used the fact that  $PF = F$ . Our discussion can be most clearly made by thinking in terms of the configuration space of the  $N$  atoms, and so the notation in Eq. (50) has been chosen accordingly. The  $3N$ -tuplets  $p$  and  $p_x$  are the representative points of the system in configuration space corresponding to the original and exchanged equilibrium arrangements of the atoms, respectively. The function  $\phi$  is localized about  $p$ ;  $P\phi$  about  $p_x$  (see Fig. 3). The number  $d_P$  is the distance between  $p$  and  $p_x$ . The  $\delta$  function in Eq. (49) specifies a hypersurface  $\Sigma$  midway between  $p$  and  $p_x$ , and the variable  $u_1$  indicates the position of the representative point of the system along the coordinate axis connecting  $p$  and  $p_x$ .

It should be clearly understood what conventions we are using in Eq. (49) and throughout this paper. As relates to the sign of the frequencies, all are given by Eq. (45), regardless of the parity of the permutation  $P$  describing the process. For our

approximation to the home-base function, Eq. (45) reduces to Eq. (49) which yields *negative* numbers for *all* frequencies. The fact that triple and pair exchange favor ferro- and antiferromagnetism, respectively, in solid  $^3\text{He}$ , has been explicitly incorporated by means of the alternating signs in front of the exchange Hamiltonians in Eqs. (37)–(39). As far as conventions which affect the magnitude of the frequencies, we are using the “standard” convention for the pair frequencies, i. e.,  $\frac{1}{2}(\epsilon_{ij}^+ - \epsilon_{ij}^-)$  where  $\epsilon_{ij}^+$  and  $\epsilon_{ij}^-$  are appropriately defined singlet and triplet energies for the pair  $(i, j)$ . The corresponding convention is used for the higher-order frequencies.

It is convenient to divide the effects which determine the size of the exchange frequencies into three types: (1) The dominant contribution arises from the Gaussian overlap and depends solely on the distance in configuration space between the original and the exchanged configurations. (2) Because of their hard cores, the exchanging atoms must maneuver around each other in the exchange process. This makes the exchange more difficult and decreases the frequency. (3) The exchange takes place within the “cage” formed by the hard cores of the surrounding neighbors, which further inhibits the process.

The important factor arising from the overlap of the Gaussian parts of  $\phi$  and  $P\phi$  may be taken out of the integral in Eq. (49):

$$J_P = -\frac{\hbar^2 A}{2m} d_P e^{-Ad_P^2/4} \frac{\int d\tau \delta(u_1) \phi_{av}^2}{\int d\tau \phi^2}, \quad (51)$$

$$\phi_{av} = \prod_i e^{-A(\vec{r}_i - \vec{R}_i^{av})^2/2F}, \quad (52)$$

$$\vec{R}_i^{av} = \frac{1}{2}(\vec{R}_i + P\vec{R}_i).$$

In fact, if one were to neglect the short-range correlations altogether, Eq. (51) would be

$$J_P = -(\hbar^2/2m) d_P A^{3/2} \pi^{-1/2} e^{-Ad_P^2/4}. \quad (53)$$

Thus no matter how complex a given exchange process is, the important matter as far as the Gaussian part of  $\phi$  is concerned, is simply  $d_P$ , the *distance in configuration space between the original and the exchanged configurations*. The general nature of this statement must be qualified somewhat, as the surface integral itself is not a valid approximation to  $J_P$  for many exchange processes, e. g., pairs and triplets composed of distant atoms, and exchanges involving large numbers of atoms. Even so, since the overlap integral  $\langle \phi | P | \phi \rangle$  is  $e^{-Ad_P^2/4}$  in this approximation, Eq. (53) is still a useful indication of the size of the frequencies for these more complex exchanges.

We report calculations of Eq. (53) for the largest exchange frequencies in the fourth column ( $J_I$ ) of Table IV, taking  $A = 1.30 \text{ \AA}^{-2}$  and the near-neighbor

distance  $\Delta = 3.75 \text{ \AA}$ . The various pair- and triple-exchange processes are identified according to the notation introduced in Fig. 1. In specifying the cyclic quadruple processes, the first four numbers in parentheses (the notation in Fig. 1) indicate the sides of the four-sided figure traced out by the atoms in the course of their exchange. This information is supplemented by the immediately following two numbers in parentheses which indicate the remaining two “diagonal” lengths of the figure. The quantity  $ZN$ , where  $Z$  is given in the table, is the number of each kind of process contributing to the total energy of the  $N$ -atom solid. For pair and triple exchange,  $ZN$  is just the number of pairs or triples of atoms of a given kind which occur in the sums over  $i < j < \dots$  in Eqs. (37)–(38). For cyclic quadruple exchange, there are three possible cyclic exchanges for each given quadruple of atoms, corresponding to the three terms in Eq. (39). Thus for example, the notation (1111), (22) and (1212), (11) refers to the same quadruples. There are  $6N$  of them. Among the four atoms of any one of these, there is one possible (1111) cyclic exchange ( $Z=6$ ) and two possible (1212) cyclic exchanges ( $Z=12$ ). All of the other cyclic quadruple processes listed correspond to different kinds of quadruples, and have only one cyclic process possible of the kind indicated by the

TABLE IV. Calculations of the most-important exchange frequencies in various approximations.  $J_I$  is calculated in each case without short-range correlations,  $J_{II}$  with just the correlations between exchanging atoms, and  $J_{III}$  with all of the correlations. These numbers are in degrees Kelvin. The exchange processes are identified according to the notation shown in Fig. 1. The additional pair of numbers included for each quadruple process specifies the two diagonal lengths. The number  $d_P$  is the distance in configuration space between the representative points of the initial and exchanged arrangements, in units of the near-neighbor distance. There are  $ZN$  processes of each kind contributing to the energy of the  $N$ -atom system.

Process	$d_P$	$Z$	$J_I$	$J_{II}$	$J_{III}$
Pair					
(1)	1.42	4	$-3.8 \times 10^{-3}$	$-1.4 \times 10^{-4}$	$-5.2 \times 10^{-5}$
(2)	1.63	3	$-2.1 \times 10^{-4}$	$-7.6 \times 10^{-6}$	$-1.2 \times 10^{-6}$
(3)	2.31	6	$-1.5 \times 10^{-9}$		
Triple					
(112)	1.83	12	$-1.1 \times 10^{-5}$	$-2.0 \times 10^{-6}$	$-9.4 \times 10^{-7}$
(113)	2.16	12	$-3.0 \times 10^{-8}$		
(223)	2.31	12	$-1.5 \times 10^{-9}$		
Cyclic quadrupole					
(1111), (22)	2.00	6	$-5.8 \times 10^{-7}$		
(1111), (23)	2.00	6	$-5.8 \times 10^{-7}$		
(1212), (11)	2.16	12	$-3.0 \times 10^{-8}$		
(1212), (14)	2.16	12	$-3.0 \times 10^{-8}$		
(1122), (13)	2.16	24	$-3.0 \times 10^{-8}$		
(2222), (33)	2.31	3	$-1.5 \times 10^{-9}$		

first four numbers in parentheses. For these processes, then,  $ZN$  is just the number of quadruples of the given kind which occur in the sum over  $i < j < k < l$  in Eq. (39). There are no double-pair quadruple processes listed in the table. Although the largest frequencies of the cyclic and double-pair types are of the same size in the approximation given by Eq. (53), we shall see shortly that the short-range correlations have a much more severe effect on the latter, and thus the dominant quadruple processes should be the cyclic ones.

The usefulness of the calculation of Eq. (53) as shown in Table IV, is that the short-range correlations will invariably reduce these results in size. Thus, one may immediately see which of the higher-order exchange processes are clearly negligible and which might be important. The striking feature of the results is how rapidly the higher-order exchange frequencies fall off in size, while the weight fact  $Z$  has not substantially increased. This suggests that the expansion for the exchange Hamiltonian in solid  $^3\text{He}$  does indeed rapidly converge. As a specific illustration, note that the collection of spin operators describing each higher-order exchange process contains some bilinear combinations of the spins which may be regrouped in the pair-exchange Hamiltonians in the manner of the renormalization of the pair frequencies described in Sec. II. Knowing the form of the higher-order exchange Hamiltonians and the numbers  $Z$ , we have all the information needed to determine the extent of this renormalization. [Consider the (112) triple process. The  $12N$  triangles contribute  $24N$  (1) neighbor pair and  $12N$  (2) neighbor pair bilinear spin products. Since there are only  $4N$  and  $3N$  distinct (1) and (2) neighbor pairs, respectively, this immediately yields Eq. (4).] For the renormalized (1) and (2) pair Hamiltonians we have

$$H_X = -2\Lambda_1 \sum_{i < j}^{\langle nn \rangle} \vec{I}_i \cdot \vec{I}_j - 2\Lambda_2 \sum_{i < j}^{\langle nnn \rangle} \vec{I}_i \cdot \vec{I}_j,$$

where

$$\Lambda_1 = J_1 - 6J_{112} + 6J_{1111} - 6J_{113} + \frac{39}{2}J_{1122} + \dots,$$

$$\Lambda_2 = J_2 - 4J_{112} + 3J_{1111} + 16J_{1122} - 8J_{223} + 2J_{2222} + \dots$$

Using the results from Eq. (53) it is clear that there is indeed extremely rapid convergence of these series. It is apparent that the (1) and (2) pair and the (112) triple processes are likely to be the only important ones in solid  $^3\text{He}$ . The only other processes even remotely close in size are the (1111) cyclic four-particle exchanges. We have not evaluated these integrals with correlation functions, though we would expect their effect in this case to be similar to that of the (112) triple process, in which case the (1111) quadruple ex-

changes should be negligible. This matter is perhaps worth checking more carefully, as the quadruple processes introduce four-spin terms into the exchange Hamiltonian, and recent results of Osheroff *et al.*<sup>32</sup> suggest that the magnetic ordering in bcc  $^3\text{He}$  is not quite as simple as it has been thought to be.

We now investigate the effect on the exchange frequencies, of the short-range correlations between exchanging atoms. We confine our attention to the (1) and (2) pair, and the (112) triple cases. Intuitively, the effect is simply that the most important routes of exchange for a system described purely by Gaussians, may involve atoms passing "through" each other to some extent (see Fig. 1). For a system of hard-sphere atoms, such routes cannot contribute to the integral, and so the exchange frequency will be reduced in size. To understand the actual manner in which the integral is affected, note that the short-range correlations serve basically to drive  $\phi$ , and thus  $\phi P \phi$ , to zero in regions of configuration space where two or more atoms are closer to each other than the hard-core distance  $\sigma$ . If such regions coincide with those where the Gaussian overlap in  $\phi P \phi$  is large, the exchange integral can be severely reduced over that calculated in the absence of the correlations. This is precisely what happens. The Gaussian overlap is large near the midpoint between  $p$  and  $p_x$  in Fig. 3, as can be seen by the fact that  $\phi P \phi$  is just a constant multiplying  $\phi_{av}^2$ . In the case of pair exchange, this corresponds to the two atoms sitting on top of one another and midway between the two lattice sites (see Fig. 4). The function  $\phi P \phi$  is, of course, driven to zero in precisely this region of configuration space owing to the short-range correlation between the two atoms. Contributions to the integral in Eq. (51) must come from further out on the "tail" of the Gaussian part of  $\phi_{av}^2$ , where the two atoms are separated by a distance of  $\sigma$  or more. The relevant Gaussian part of  $\phi_{av}^2$  is  $e^{-A r^2/2}$ , where  $\vec{r}$  is the relative coordinate for the two atoms. Thus for *any* pair exchange, the effect of the short-range correlation between the two atoms is to reduce the exchange frequency by a factor of  $e^{A\sigma^2/2}$ . This factor is about  $\frac{1}{25}$  for  $A = 1.30 \text{ \AA}^{-2}$ . [Actually, the Nosanow correlation function is roughly equivalent in these exchange integrals to  $\Theta(r - \rho)$ , where  $\rho = 2.25 \text{ \AA}$ . Thus, one should evaluate  $e^{-A\rho^2/2}$ .]

The effect of the short-range correlations among exchanging atoms is less severe for triple exchange. In this case the Gaussian part of  $\phi_{av}^2$  is large when the three atoms are near the midpoints of the sides of the triangle determined by the three lattice sites, as shown in Fig. 4. In contrast to the pair-exchange case, part of the region of large Gaussian overlap is not eliminated by the correla-

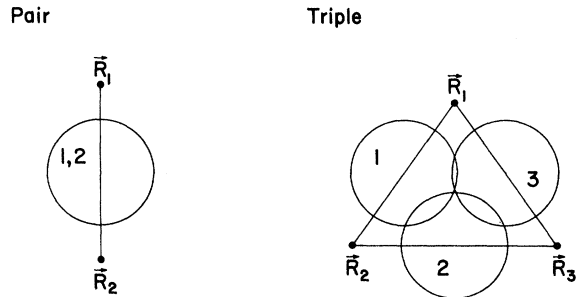


FIG. 4. Effect of the short-range correlations between the exchanging atoms on the (1) pair and (112) triple-exchange processes. The Gaussian part of  $\phi P\phi$  is large when the atoms are located nearby the positions shown here, relative to the lattice sites  $\bar{R}_i$ . The atoms are drawn as spheres of diameter  $\sigma$  to illustrate the effect of the short-range correlations, which is basically to drive  $\phi P\phi$  to zero when any two spheres overlap. Thus contributions to the pair-exchange integrals must come from further out on the tail of the Gaussian part of  $\phi P\phi$  where the two atoms are separated by a distance of  $\sigma$  or more. This leads to a reduction of the integral by a factor of  $e^{-A\sigma^2/2} \approx \frac{1}{25}$  for  $A = 1.3 \text{ \AA}^{-2}$ . Dominant contributions to the triple-exchange integral come from configurations in which any of the atoms may be displaced further out from, but not in closer to, the center of the triangle. This leads to a reduction by a factor on the order of  $(\frac{1}{2})^3 = \frac{1}{8}$ .

tions, as can be seen from the fact that the atoms need only be displaced slightly away from the center of the triangle in order to avoid each other's hard cores. The atoms have been drawn as spheres of diameter  $\sigma$  in Fig. 4 to illustrate this fact. Guyer and Zane have mistakenly argued that this implies the effect of these short-range correlations on triple exchange is negligible. This is not the case. A crude estimate may be obtained as follows: Note that the Gaussian part of  $\phi_{av}^2$  for each atom, namely  $e^{-A(\tau_i - \bar{R}_i^{av})^2}$ , lies half on each side of the appropriate side of the triangle. Yet, roughly speaking, only if each of the three atoms lies outside the triangle will one get contributions to the integral in Eq. (51). Thus one might expect the effect to be a factor of  $(\frac{1}{2})^3 = \frac{1}{8}$  reduction in size. Numerical computation of Eq. (51) for  $A = 1.30 \text{ \AA}^{-2}$  and  $\Delta = 3.75 \text{ \AA}$ , including only the short-range correlations among the three atoms, shows the (112) triple frequency reduced by a factor of  $\frac{1}{5}$  over that calculated without these correlations. These results, as well as those for the (1) and (2) pair cases keeping only the short-range correlation between the pair, are given in the fifth column ( $J_{II}$ ) of Table IV. It is on the basis of these numbers, that we suggest the dominant four-particle processes are the cyclic ones. For example, as the relevant geometries are somewhat similar, we would expect the effect of the short-range correlations among the four atoms undergoing the

cyclic (1111) exchange to be of the same order of magnitude as that for the (112) triple process, i. e., a factor  $O(\frac{1}{5})$ . The corresponding double-pair (1, 1) process, however, involves two pair overlaps, and so the effect in this case is likely to be  $O(\frac{1}{25})$ .

We turn now to the last of the three effects mentioned previously, that due to the short-range correlations between the exchanging atoms and their surrounding neighbors. It has been pointed out elsewhere<sup>17</sup> that this effect is quite important, though it has been ignored in nearly all the existing exchange calculations in solid  $^3\text{He}$ , including the estimates of Zane. A simple drawing can show why these correlations are important. In Fig. 5 we show the relative arrangement of the exchanging atoms and some of their neighbors, for the cases of the three most important exchange processes. The atoms are drawn as spheres of diameter  $\sigma$ , as the significance of the short-range correlation functions is basically that the atoms should be treated as impenetrable spheres of this size. We have already discussed the reduction in size of the frequencies which follows from the necessity of the exchanging atoms maneuvering around each other in the process of exchange. It is clear from Fig. 5 that the processes will be further inhibited by the necessity of their taking place within the rather limited confines of the "cage" composed of the hard cores of the surrounding neighbors. One should not be misled by the possibility in each case of choosing particular routes in which the exchanging atoms do not encounter their neighbors. Roughly speaking, the exchange integral represents the net effect of all possible routes available to the system. By including the short-range correlations with neighboring atoms, some of the routes which would otherwise have been possible for the system, are eliminated, and thus the frequency is reduced in size. Analysis of the exchange integrals with these additional correlation functions is sufficiently complex, that it is not very illuminating to try to put this intuitive discussion into more rigorous form. Instead we shall immediately turn to the results of numerical calculations, and present them in such a way as to show which neighboring atoms are important in each case, and how large the effect is. We have used a greatly improved version of the Monte Carlo technique described elsewhere<sup>17</sup> to do the integrals. We discuss this technique in Appendix B.

The idea of hard-core interactions among the atoms suggests that the short-range correlations between the exchanging atoms and their neighbors should be less important to the integral the farther these neighbors are from the local region where the exchange takes place. To this end, we have grouped the neighboring atoms in shells, in each

case according to their distance from the center of mass of the two or three exchanging atoms (see Fig. 6). One may then evaluate a series of cluster approximations to Eq. (51) in which the short-range correlations are retained only among a group of atoms including and centered about the exchanging atoms. That is, one replaces  $F$  by

$$\prod_{1 \leq i < j \leq n} f(r_{ij}) \quad (54)$$

in both numerator and the normalization denominator of Eq. (51), where we assume the atoms to be numbered 1, 2, ... beginning with the exchanging atoms and then working outwards through consecutive shells of the neighboring atoms. In the case of (1) pair exchange, for example, taking  $n=2$  retains only the correlation between the two exchanging atoms. The next choice is clearly  $n=8$ , where the additional six intermediate atoms shown

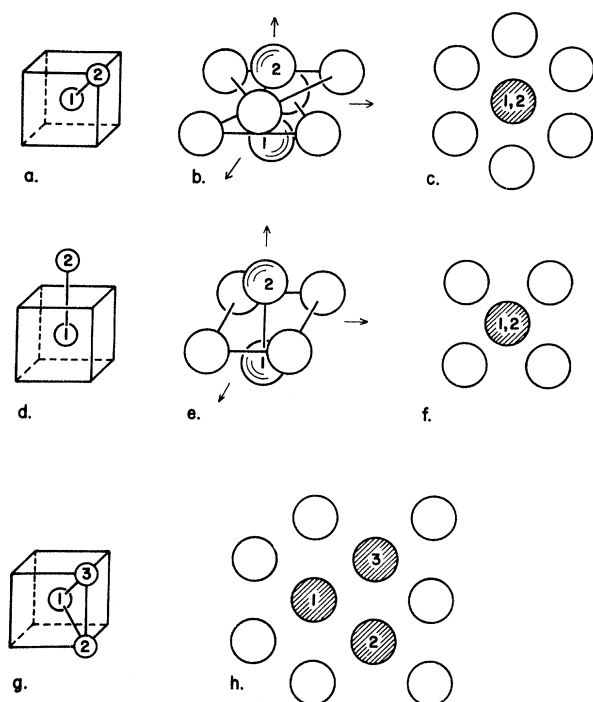


FIG. 5. Many-body contributions to pair and triple exchange (I). (a), (d), and (g): The atoms respectively involved in the (1) and (2) pair and the (112) triple processes are shown in the basic cube of the bcc structure. Some of the surrounding neighbors which form the "cage" in which these processes take place are shown in the remaining drawings. These drawings are to scale with the atoms portrayed as spheres of diameter  $\sigma$ . (b) Near-neighbor exchange occurs through two "hoops" of three atoms each lying in planes  $\frac{1}{2}$  and  $\frac{3}{2}$  the distance from atom 1 to 2. (c) Top view. (e) Next-near-neighbor exchange occurs through the center of a square of four atoms that are second neighbors of each other. (f) Top view. (h) Neighboring atoms lying in the plane of the exchanging triple are shown.

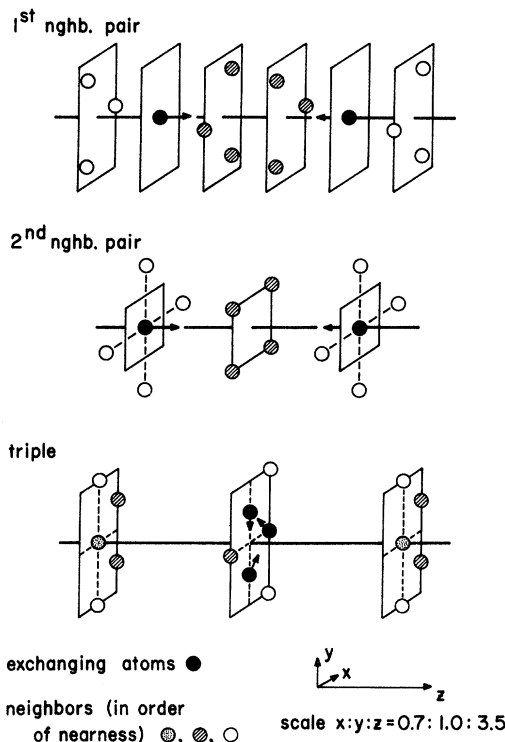


FIG. 6. Many-body contributions to pair and triple exchange (II). The geometry of the surrounding neighbors for the (1) and (2) pair and the (112) triple processes is shown in more detail.

in Fig. 6 are included in the group, and so on. (We shall subsequently refer to these integrals as  $n$ -body cluster approximations to the full integral.) The values of these cluster integrals for various choices of  $n$  are given in Tables V-VII for the (1) and (2) pair, and the (112) triple processes, respectively. These tables should be read in conjunction with Fig. 6. In all three cases it is evident that the cluster integrals converge fairly rapidly with the value of  $n$ . The results for the (1) and (2) pair cases are particularly striking. While the integrals with just the single correlation be-

TABLE V. Convergence of the  $n$ -body cluster integral for the first-neighbor pair-exchange frequency  $J_1$ . As  $n$  increases, more surrounding neighbors of the exchanging pair are included in the integral (see Fig. 6). Two cases are considered: (a)  $R=3.75 \text{ \AA}$ ,  $A=1.30 \text{ \AA}^{-2}$ ; and (b)  $R=3.45 \text{ \AA}$ ,  $A=1.60 \text{ \AA}^{-2}$ . All values of  $J_1$  are in units of  $10^{-5} \text{ }^\circ\text{K}$ .

$n$	$J_1^a$	$J_1^b$
2	-13.94	-5.67
8	-5.12 $\pm$ 0.03	-1.10 $\pm$ 0.01
14	-5.67 $\pm$ 0.02	-1.21 $\pm$ 0.02
22	-5.10 $\pm$ 0.03	-1.11 $\pm$ 0.02
40	-5.17 $\pm$ 0.10	



TABLE VI. Convergence of the  $n$ -body cluster integral for the second-neighbor pair-exchange frequency  $J_2$ . As  $n$  increases, more surrounding neighbors of the exchanging pair are included in the integral (see Fig. 6). Two cases are considered: (a)  $R=3.75 \text{ \AA}$ ,  $A=1.30 \text{ \AA}^{-2}$ ; and (b)  $R=3.45 \text{ \AA}$ ,  $A=1.60 \text{ \AA}^{-2}$ . All values of  $J_2$  are in units of  $10^{-7} \text{ }^\circ\text{K}$ .

$n$	$J_2^a$	$J_2^b$
2	-75.7	-26.78
6	-12.7 $\pm$ 0.1	-1.52 $\pm$ 0.01
14	-11.1 $\pm$ 0.2	-1.49 $\pm$ 0.05
22	-11.9 $\pm$ 0.4	-1.50 $\pm$ 0.04

tween the exchanging atoms are clearly inadequate, one need only include the additional correlations with the six and four intermediate atoms, respectively, to get the result of the full integral to within a few percent. This is intuitively quite sensible, for it is precisely these atoms which in some sense are the neighbors which directly get in the way of the two exchanging atoms. The results for the (112) triple process converge somewhat more slowly with  $n$ . Perhaps this is because it is not so much that there are key neighboring atoms which directly interfere with the exchange, but rather that the region in which the process may take place is somewhat restricted by the totality of the immediate neighbors. In any case, when  $n$  is as large as 10, i. e., the three exchanging atoms and the seven closest neighbors are included, the cluster integral appears to have converged to within about 10% of the value of the full integral. For the choice of  $A=1.30 \text{ \AA}^{-2}$  and  $\Delta=3.75 \text{ \AA}$  the effect of the neighboring atoms is seen to be a reduction of the exchange frequencies by factors of about  $\frac{1}{3}$ ,  $\frac{1}{6}$ , and  $\frac{1}{2}$ , respectively, for the (1) and (2) pair and the (112) triple processes. These effects are by no means small, as we have emphasized. They are extremely sensitive to the parameters  $A$  and  $\Delta$ . Given the range of  $A$  values taken at each density in the current literature, the above choice represents a relatively tight single-particle Gaussian. For contrast, we have also evaluated the cluster integrals for  $\Delta=3.45 \text{ \AA}$  and  $A=1.60 \text{ \AA}^{-2}$ , which corresponds to a relatively broad Gaussian given the current  $A$  values taken at this higher density. In this case, the above factors are  $\frac{1}{5}$ ,  $\frac{1}{17}$ , and  $\frac{1}{3}$ , respectively, for the three processes. In general, it appears that the effects of the neighboring hard cores are least severe for the (112) triple process and most severe for the (2) pair process. The fact that the effects are more severe for the (2) pair than for the (1) pair process can be understood in that for the former, the four intermediate atoms are second neighbors of each other, as contrasted with intermediate neighbors (in a given plane) for the latter being third neighbors of each

other. Views along the axis of the exchanging atoms in Figs. 5(c) and 5(f) show there to be "more room" in the "cage" for the (1) pair exchange than for the (2) pair exchange.

In all of this discussion, one should bear in mind that the numerical results on which it is based have been obtained with the Nosanow correlation function—a function which levels off well before the near-neighbor distance. In the case of correlation functions for which this is not true, such as  $f(r) = e^{-(B/r)^{5/2}}$  used by Hansen and Levesque,<sup>31</sup> for example, the cluster integrals for the (1) pair frequency will not begin to converge until all first neighbors of the two atoms are included. Although we expect generally the same qualitative features as previously described, this becomes a more complex problem numerically. These correlation functions serve not only to represent the hard-core repulsion between atoms but, in addition, play an important role in determining the extent to which the atoms are localized about their lattice sites. This latter role is taken almost completely by the single-particle functions when Nosanow-like correlation functions are used.

We would now like to present calculated results for the size and density dependence of the various frequencies. Unfortunately, there is no clear agreement in the literature as to what  $A$  values and correlation functions should be used. The  $A$  values (in some cases extrapolated) taken in some of the exchange calculations in solid  $^3\text{He}$  are given in Table VIII. Accordingly, we have performed Monte Carlo calculations of Eq. (49) for the (1) and (2) pair, and the (112) triple frequencies for a range of  $A$  values at each of four densities. Since the effect of the different correlation functions used by the workers listed in this table is expected to be much less important,<sup>17</sup> we have used the numerically convenient Nosanow correlation given by Eq. (48) in all calculations. These results are reported in Table IX and Figs. 7 and 8. The calculations were done taking  $n=8, 6,$  and  $10,$  respectively, for the three processes. Since the

TABLE VII. Convergence of the  $n$ -body cluster integral for the largest triple-exchange frequency  $J_{112}$ . As  $n$  increases, more surrounding neighbors of the exchanging triple are included in the integral (see Fig. 6). Two cases are considered: (a)  $R=3.75 \text{ \AA}$ ,  $A=1.30 \text{ \AA}^{-2}$ ; and (b)  $R=3.45 \text{ \AA}$ ,  $A=1.60 \text{ \AA}^{-2}$ . All values of the  $J_{112}$  are in units of  $10^{-7} \text{ }^\circ\text{K}$ .

$n$	$J_{112}^a$	$J_{112}^b$
3	-20.3 $\pm$ 0.1	-7.28 $\pm$ 0.04
5	-15.3 $\pm$ 0.1	-5.54 $\pm$ 0.12
10	-10.4 $\pm$ 0.1	-2.30 $\pm$ 0.05
16	-8.72 $\pm$ 0.21	-2.05 $\pm$ 0.06
26	-9.35 $\pm$ 0.23	-2.52 $\pm$ 0.08

TABLE VIII. Gaussian parameter  $A$  at various values of the near-neighbor distance  $R$  as extrapolated from the values used by Nosanov and Mullin (NM), Guyer and Zane (GZ), Ebner and Sange (ES), and Ostgaard (O). All values of  $A$  are in  $\text{\AA}^{-2}$ .

$R$ ( $\text{\AA}$ )	3.45	3.55	3.65	3.75
$A$ (NM)	1.73	1.59	1.44	1.30
$A$ (GZ)	2.23	1.90	1.60	1.32
$A$ (ES)	1.95	1.63	1.41	1.20
$A$ (O)	2.15	1.71	1.38	1.10

statistical scatter for each Monte Carlo calculation was typically a few percent, the accuracy of these results is determined largely by the convergence properties with  $n$ , as exhibited in Tables V–VII. We expect the results to be within about 5% of the value of the full integral for the pair frequencies and within about 10% for the triple frequency. In Figs. 7 and 8, it is seen that the dependence of the exchange integrals on  $A$ , at a fixed density, is very nearly exponential, thus allowing easy extrapolation of these results to any intermediate  $A$  values. We present the values of the exchange

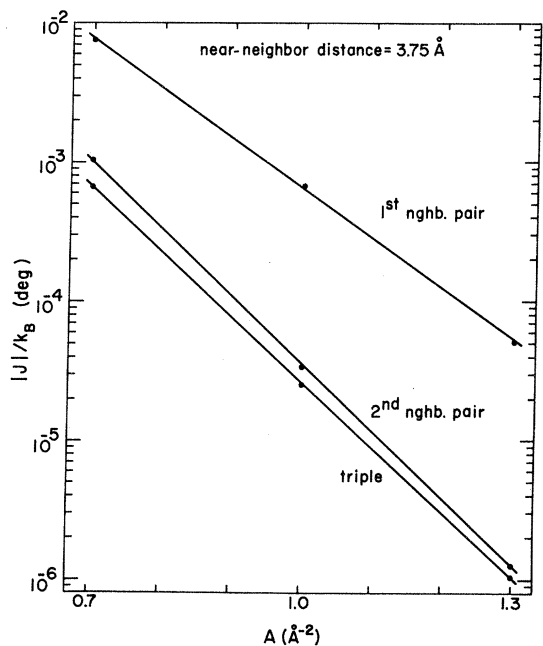


FIG. 7. Exchange constants  $J$  (in degrees Kelvin) at a molar volume of  $24.7 \text{ cm}^3/\text{mole}$  (near-neighbor distance  $\Delta = 3.75 \text{ \AA}$ ). The results of the full many-body calculation of  $J_1$  (first-neighbor pair),  $J_2$  (second-neighbor pair), and  $J_{112}$  (triple) are shown as a function of the Einstein parameter  $A$ . The qualitative result is  $|J_1| \gg |J_2| \gg |J_{112}|$ . As a consequence the effective next-neighbor pair-exchange constant  $\Lambda_2$  of Eq. (6) is ferromagnetic. Note that the ratios  $|J_1|/|J_2|$  and  $|J_2|/|J_{112}|$  are a mild function of  $A$  while  $|J_1|$ ,  $|J_2|$ , and  $|J_{112}|$  change by three orders of magnitude.

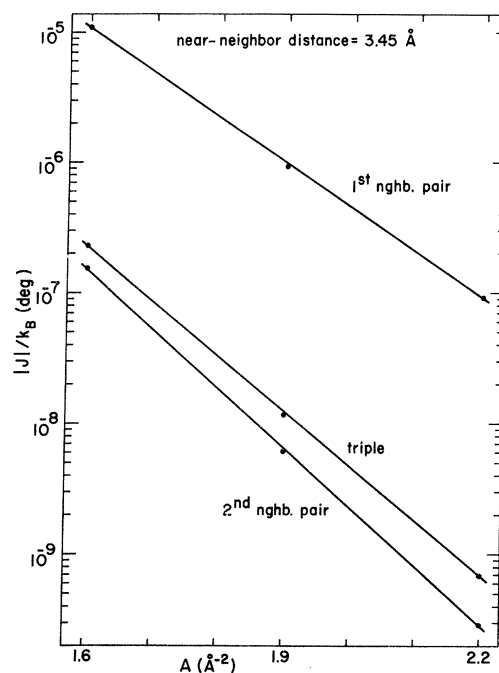


FIG. 8. Exchange constants  $J$  (in degrees Kelvin) at a molar volume of  $20.0 \text{ cm}^3/\text{mole}$  (near-neighbor distance  $\Delta = 3.45 \text{ \AA}$ ). The results of the full many-body calculation of  $J_1$ ,  $J_2$ , and  $J_{112}$  are shown as a function of  $A$ . The comments in the caption to Fig. 7 apply here.

frequencies determined in this manner for the Guyer–Zane, and for the Ebner–Sung choices of  $A$ , in Fig. 9. These two sets of  $A$  values more or less represent the extremes occurring in Table VIII, aside from those used by Nosanov and co-workers which may exhibit<sup>17</sup> an unrealistically “flat” density dependence.

The results for  $J_1$  in Fig. 9 are of about the right density dependence, but even the best is a factor of 6 smaller in magnitude than experiment. We shall address this problem a bit later. (We must also show, for example, that Panczyk and Adams<sup>6</sup> are essentially measuring  $J_1$ .) The important point for the moment is that we will be unable to conclusively determine the ratio  $J_{112}/J_1$  which is so important to the discussion of Sec. II. Thus, at the density corresponding to  $\Delta = 3.75 \text{ \AA}$  the choice of  $A$  taken by Ebner and Sung leads to a value of  $\frac{1}{40}$  for this ratio. On the other hand, if one takes the  $A$  value at this density for which the calculated  $J_1$  agrees with experiment, i. e.,  $A \approx 1.0 \text{ \AA}^{-2}$ , then this ratio becomes more like  $\frac{1}{20}$ . While the former value is clearly too small, the latter comes somewhat closer to the ratio  $\frac{1}{15}$  indicated in Sec. II as being necessary to explain the results of Kirk and Adams.<sup>18</sup> Unfortunately, picking the  $A$  value by fitting the (1) pair results to experiment is phenomenology. In spite of these uncertainties, however, there are certain conclu-

TABLE IX. Exchange frequencies at various densities and for various Gaussian values.  $J_1$ ,  $J_2$ , and  $J_{112}$  are the first-neighbor pair-, second-neighbor pair-, and the largest triple-exchange frequency, respectively. They were calculated with the 8, 6, and 10 atom cluster integrals, respectively.  $R$  is the near-neighbor distance and  $A$  is the Gaussian parameter. All frequencies are in degrees Kelvin.

$R$ (Å)	$A$ (Å <sup>-2</sup> )	$J_1$	$J_2$	$J_{112}$
3.75	1.30	$-5.12 \times 10^{-5}$	$-1.27 \times 10^{-6}$	$-1.04 \times 10^{-6}$
	1.00	$-6.69 \times 10^{-4}$	$-3.41 \times 10^{-5}$	$-2.53 \times 10^{-5}$
	0.70	$-7.63 \times 10^{-3}$	$-1.04 \times 10^{-3}$	$-6.74 \times 10^{-4}$
3.65	1.60	$-5.81 \times 10^{-6}$	$-6.52 \times 10^{-8}$	$-6.24 \times 10^{-8}$
	1.00	$-7.73 \times 10^{-4}$	$-5.08 \times 10^{-5}$	$-3.67 \times 10^{-5}$
3.55	1.90	$-6.95 \times 10^{-7}$	$-4.25 \times 10^{-9}$	$-6.14 \times 10^{-9}$
	1.30	$-8.35 \times 10^{-5}$	$-2.69 \times 10^{-6}$	$-2.61 \times 10^{-6}$
3.45	2.20	$-9.33 \times 10^{-8}$	$-2.92 \times 10^{-10}$	$-6.98 \times 10^{-10}$
	1.90	$-9.32 \times 10^{-7}$	$-6.07 \times 10^{-9}$	$-1.18 \times 10^{-8}$
	1.60	$-1.10 \times 10^{-5}$	$-1.52 \times 10^{-7}$	$-2.30 \times 10^{-7}$

sions that follow clearly from our results. Over the whole range of densities and  $A$  values we have investigated,  $J_{112}$  is either approximately equal to or at most a factor of 2 larger than  $J_2$ . The effective second-neighbor exchange frequency defined in Sec. II,  $\Lambda_2 = J_2 - 4J_{112}$ , is thus clearly ferromagnetic. The effect of the higher-order exchange frequencies in bcc <sup>3</sup>He is, therefore, in the right direction to explain the Kirk and Adams results. We are also able to determine the magnetic Grüneisen constants for the various frequencies. We do so for the lower densities ( $\Delta = 3.65 - 3.75$  Å) taking the Ebner-Sung  $A$  values, as these lead to a density dependence for  $J_1$  in best agreement with experiment. We find  $d \ln |J_1| / d \ln V = 18.0$ ,  $d \ln |J_2| / d \ln V = 23.5$ ,  $d \ln |J_{112}| / d \ln V = 22.9$ ,  $d \ln |\Lambda_1| / d \ln V = 17.7$ , and  $d \ln |\Lambda_2| / d \ln V = 21.9$ . These values are good to about  $\pm 1.0$ . The estimates of Zane<sup>16</sup> are thus somewhat too large for  $d \ln |J_{112}| / d \ln V$  and too small for  $d \ln |J_2| / d \ln V$ .

Our results illustrate certain more general features relating to the density dependence of the frequencies, which are worth mentioning. It is well known that the implicit density dependence of the frequencies through the parameter  $A$  dominates the explicit dependence through  $\Delta$ . That is, if  $\Delta$  is increased, the exchange process is enhanced far more by the fact that the atoms may be found farther away from their lattice sites (the parameter  $A$ ) than it is inhibited by the fact that the atoms have a slightly larger distance to go in order to exchange (the parameter  $\Delta$ ). We illustrate the dependence of the frequencies on these two parameters in Fig. 10. We have taken the results for the frequencies as functions of  $A$  at the two density extremes, and included them on the same plot, extrapolating the curves over the full range of  $A$  values in each case. For the (1) pair frequency, for example, the parameter  $A$  is seen to govern

a five-order-of-magnitude change, while  $\Delta$  causes the frequency to be changed by only about a factor of 2. To within a factor of 2, then, the density dependence of  $J_1$  is seen to be completely due to that of the parameter  $A$ .

To facilitate a comparison of theory and experiment, we now briefly comment on the measurements of Panczyk and Adams.<sup>6</sup> According to the analysis in Sec. II, they have measured a quantity  $J$ , defined by

$$J^2 \frac{d \ln |J|}{d \ln V} = \Lambda_1^2 \frac{d \ln |\Lambda_1|}{d \ln V} + \frac{3}{4} \Lambda_2^2 \frac{d \ln |\Lambda_2|}{d \ln V}, \quad (55)$$

where

$$\Lambda_1 = J_1 - 6J_{112}, \quad \Lambda_2 = J_2 - 4J_{112}.$$

Except for unrealistically small  $A$  values near  $A = 0.7$  Å<sup>-2</sup>, we find that  $\Lambda_2$  is generally an order of magnitude smaller than  $\Lambda_1$  for the whole range of densities and  $A$  values we have investigated. Since the various magnetic Grüneisen constants are roughly of the same size, it is clear that Panczyk and Adams have measured essentially  $\Lambda_1$ , which is in turn within 20% or so of  $J_1$  itself. Thus, it

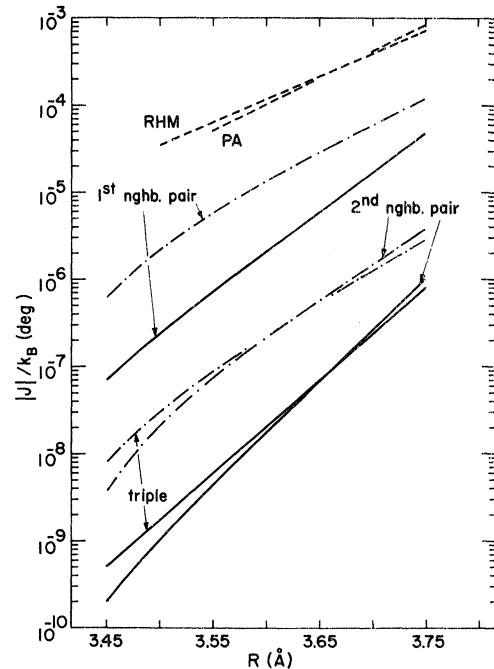


FIG. 9. Exchange constants as a function of near-neighbor distance  $R$ . The dashed lines are the experimental values of  $J_1$  from the thermodynamic data of Panczyk and Adams (PA) and the NMR data of Richardson, Hunt, and Meyer (RHM). The remaining curves are theoretical results for  $J_1$ ,  $J_2$ , and  $J_{112}$  obtained using the values of the Einstein parameter due to Ebner and Sung (dash-dot lines) and Zane and Guyer (solid lines); see Table VIII. Note that even the best theoretical values for  $J_1$  are about a factor of 6 smaller than experiment. See the discussion in the text, below Eq. (55), on this point.

is valid to compare our calculated results for  $J_1$  to these experimental results as is done in Fig. 9.

We conclude this section by discussing the discrepancies between our theoretical results for  $J_1$  and experiment. Even the most favorable  $A$  values in Table VIII lead to magnitudes for  $J_1$  about a factor of 6 smaller than experiment. Furthermore, we expect the Nosanow correlation, which was used in these calculations, to give a larger magnitude for the exchange frequencies than would be given by the other correlation functions. This has been explicitly demonstrated at least at the level of the two-body cluster approximation.<sup>17</sup> In the crucial region  $2\text{\AA} < r < 3\text{\AA}$ , the Nosanow correlation has the "softest" hard core of these various correlation functions. This is also true of the Ostgaard correlation, which falls between that of Nosanow and that of Ebner-Sung in this region.<sup>17</sup> It has been noted elsewhere<sup>17</sup> that the tendency for theoretical calculations of  $J_1$  to come out too small is often obscured in the literature by calculations which neglect the short-range correlations

between the exchanging atoms and their neighbors. For example, the two-body cluster approximation to Eq. (49), which also neglects these correlations, yields about the same result as obtained by Ostgaard<sup>16</sup> when his (extrapolated)  $A$  value is used at low density. The full integral is reduced by a factor of 3. At this density extreme, Ostgaard's  $A$  values are somewhat smaller than those of Ebner and Sung, from which the higher  $J_1$  curve in Fig. 9 was obtained.

We have argued previously that the many-body surface integral given by Eq. (45) will give the correct result for  $J_1$  to first order if the true home-base function is used. The general tendency for theoretical calculations of  $J_1$  to be too small seems to suggest that the usual approximation to the home-base function is not adequate. We feel, however, that there is still too much uncertainty in the lattice-dynamical calculations for solid <sup>3</sup>He to discredit use of Eq. (47) in exchange calculations. For example, there is one lattice-dynamical calculation which is radically different from those on which the workers listed in Table VIII have based their exchange calculations. Hansen and Levesque<sup>31</sup> have used Eq. (47) with

$f(r) = e^{-B/r} r^{5/2}$  and obtained  $A$  values generally less than half the size of those in Table VIII. Such small  $A$  values are possible in their calculation because the correlation function rises very slowly to unity, and thus plays an important role in determining the localization of the atoms about the lattice sites. In preliminary calculations of the many-body surface integral with this correlation function and with smoothed fits to the Hansen-Levesque values for  $A$  and  $B$ , we find  $J_1$  of about the right density dependence, but about an order of magnitude *too large* in size.

It is entirely possible that when the lattice-dynamical calculations can agree on the choice of correlation function and the value of  $A$ , that Eq. (47) will prove inadequate for exchange calculations. Solution of the various differential equations for the correlation function cannot, in practice, correct any error in the tail of the single-particle Gaussian. As mentioned earlier, there is good reason to believe that the tail of the single-particle Gaussian is in fact too small, which is consistent with the generally small results for  $J_1$ . We do not feel that the use of an Einstein approximation to the phonons in Eq. (47) accounts for these small results, at least as calculated by the many-body surface integral. Although Nosanow and Varma<sup>12</sup> have found the inclusion of phonons to increase  $J_1$  by as much as a factor of 4 in working with a two-body cluster approximation to the many-body volume integral, we find the corresponding calculation for the surface integral to not only have a much smaller effect, but in fact, the frequency is

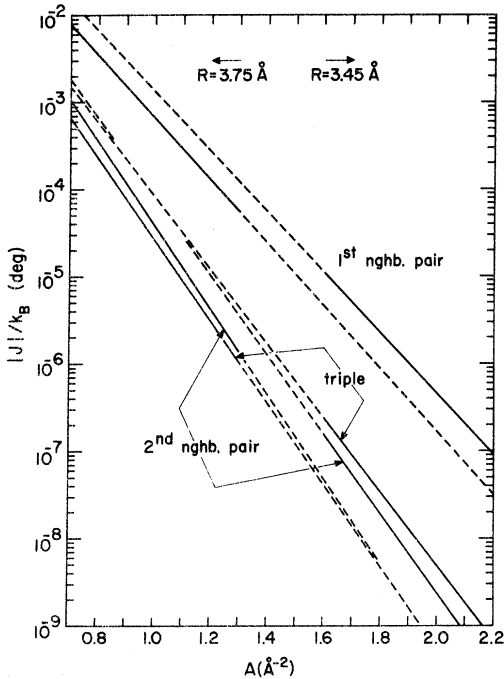


FIG. 10. Volume dependence of the exchange constants. The volume dependence of the exchange constants comes about primarily because of the volume dependence of  $A$ , a measure of the size of the single-particle density. Recall  $\langle u^2 \rangle = \frac{3}{2}A$ . To emphasize this point we have plotted  $|J_1|$ ,  $|J_2|$ , and  $|J_{112}|$  as a function of  $A$  at two different values of  $\Delta$ , 3.75 and 3.45 Å. The variation of  $J$  with  $A$  is dramatic whereas the variation of  $J$  with  $\Delta$  is about a factor of 2. At  $\Delta = 3.75$  Å a reasonable value of  $A$  is  $1.3 \text{ \AA}^{-2}$ ; at  $\Delta = 3.45$  Å a reasonable value of  $A$  is  $2.0 \text{ \AA}^{-2}$ . See Table VIII.

reduced in size. A crude estimate shows why. The two-body cluster approximation to Eq. (49) with the Einstein approximation to the phonons yields  $J_1 \sim e^{-A(\Delta^2 + \sigma^2)^{1/2}}$ , as we have discussed earlier. If the two-branch<sup>12</sup> approximation to the phonons is used, one gets  $J_1 \sim e^{-(F_{\parallel}\Delta^2 + G_{\perp}\sigma^2)}$ , where the notation is that of Nosanow and Varma. From their Table III, one sees that  $F_{\parallel}$  and  $G_{\perp}$  differ from  $\frac{1}{2}A$  by roughly the same amount, and  $G_{\perp} < \frac{1}{2}A < F_{\parallel}$ . Since  $\Delta^2 \sim 2\sigma^2$ , the coefficient of  $\Delta^2$  is more important and the frequency is accordingly decreased in size relative to the Einstein calculation. We do find, in agreement with Nosanow and Varma, that the two-branch approximation yields results of the same density dependence and about a factor of 2 larger than those obtained with the one-branch<sup>12</sup> approximation.

### V. CONCLUSIONS

In this paper we have presented a formal development of the Hamiltonian taken to describe higher-order exchange processes in solid  $^3\text{He}$ . Exact expressions for the various frequencies have been analyzed in detail to see what effects contribute to their size and to show that the exchange Hamiltonian for this solid converges rapidly. It is seen that the (1) and (2) pair-exchange processes and the (112) triple-exchange process are likely to be the only important ones. Monte Carlo calculations of the many-body surface integral expressions for these frequencies show that  $|J_1| \gg |J_2| \approx |J_{112}|$ . Because of uncertainties in the current lattice-dynamical calculations, we can only say that  $J_{112}$  is somewhat less than an order of magnitude smaller than  $J_1$ . The density dependence of  $J_{112}$  is found to be essentially the same as that of  $J_2$  and  $d \ln |J_{112}| / d \ln V \approx 1.2 d \ln |J_1| / d \ln V$ .

The significant effect of the (112) triple exchange is to renormalize the (2) pair-exchange interaction, and, in fact, to make it ferromagnetic. In analysis of the thermodynamic functions it is seen that only by measurements in nonzero magnetic fields can one hope to see the effects of the higher-order exchange processes in bcc  $^3\text{He}$ , i. e., this renormalized next-neighbor exchange interaction. However, most of these measurements will be hindered by trivial field dependences, against which it will be difficult to discern any effects of the higher-order exchange processes. Such trivial field dependence is absent in quantities involving a volume derivative. Of the current measurements, only the single experiment of Kirk and Adams is truly suited to probe the existence of higher-order exchange processes.

In sum, although both theory and experiment strongly suggest that the presence of higher-order exchanges is indeed being seen, this matter has not yet been conclusively settled.

### ACKNOWLEDGMENTS

We are pleased to acknowledge helpful discussions with L. H. Nosanow, R. C. Richardson, L. J. Zane, and William J. Mullin, and correspondence with C. Herring.

### APPENDIX A. TWO-BODY SURFACE INTEGRAL

A number of theories<sup>13-16</sup> treating first-neighbor pair exchange in solid  $^3\text{He}$  have been based on perturbation solutions of either a two-body Schrödinger equation or Bethe-Goldstone equation. They determine  $J$  as the sum of various "tunneling", "interaction", and "correlation" contributions. The purpose of this appendix is to show that the two-body surface integral for  $J$  follows rigorously from the two-body Schrödinger equation, and thus must exactly sum all of these various contributions. We state certain general conclusions which follow simply from the surface-integral treatment, but which are obscured in the above theories due to the large cancellations among the competing contributions. The terms in the Bethe-Goldstone equation which distinguish it from a two-body Schrödinger equation are associated with small corrections to the single-particle potentials. In a practical calculation, these terms have a negligible effect on the wave function and on energy differences.<sup>13</sup> Therefore, we believe the conclusions in this appendix to be also valid for theories of exchange based on the Bethe-Goldstone equation. Brandow<sup>15</sup> has, in fact, observed that the surface integral should yield a reasonable approximation to the singlet-triplet splitting of the Bethe-Goldstone equation. It should be noted that the disadvantage of working with *any* two-body equation is that the choice of single-particle potentials which are amenable to practical computation are unlikely to represent the effect of the lattice medium sufficiently realistically. In particular these calculations omit the rather sizeable effect of the many-body short-range correlations. Thus, the  $J$  we discuss in this appendix, and which the various workers calculate, is not by any means guaranteed to be the true exchange frequency. Rather it is simply half the singlet-triplet splitting of the two-body Hamiltonian one assumes to begin with.

#### 1. Exchange in Terms of "Exact" Home-Base Wave Functions

We briefly review the derivation of the two-body surface integral using a generalization of standard procedure. Consider the spin-independent two-body Hamiltonian

$$H(12) = T(1) + T(2) + W(1) + W(2) + v(12) = H(21) ,$$

where  $T(1)$  and  $T(2)$  are the kinetic-energy operators, the double-well potential  $W(\vec{r})$  has minima at lattice sites  $\vec{R}_1$  and  $\vec{R}_2$ , and where  $v(12)$  incorporates the hard-core repulsion between the two atoms. We are interested in the lowest symmetric

and antisymmetric eigenstates of  $H(12)$ , with energies  $E^+$  and  $E^-$ , respectively,

$$H\psi^+ = E^+\psi^+, \quad (56)$$

$$H\psi^- = E^-\psi^-. \quad (57)$$

As we are treating a system where exchange is small, the eigenfunctions  $\psi^+$  and  $\psi^-$  may be taken so that  $\psi^+ \simeq \psi^-$  in the "right" half of the configuration space of the pair of particles (denote this space by  $\Gamma_R$ ), and  $\psi^+ \simeq -\psi^-$  in the "left" half of the space (denoted by  $\Gamma_L$ ). The "exact" home-base functions  $\phi_R$  and  $\phi_L$ , defined by  $(\psi^+ + \psi^-)/\sqrt{2}$  and  $(\psi^+ - \psi^-)/\sqrt{2}$ , respectively, are thus mainly localized in the "right" and "left" half-spaces, respectively. The half-space  $\Gamma_R$  is defined by

$$(\vec{r}_1 - \vec{r}_2) \cdot (\vec{R}_1 - \vec{R}_2) > 0, \quad (58)$$

where  $\vec{r}_1$  and  $\vec{r}_2$  are the position vectors for the two atoms. The "right" and "left" half-spaces are separated by a five-dimensional hypersurface which we denote by  $\Sigma$  (see Fig. 11).

To obtain the surface integral, one multiplies Eq. (56) by  $\psi^{*-}$ , the complex conjugate of Eq. (57) by  $\psi^+$ , and integrates over  $\Gamma_R$ . The difference of the two resulting equations is

$$\begin{aligned} (E^+ - E^-) \int_{\Gamma_R} \psi^+ \psi^{*-} &= \int_{\Gamma_R} (\psi^{*-} H \psi^+ - \psi^+ H \psi^{*-}) \\ &= -\frac{\hbar^2}{2m} \int_{\Gamma_R} \vec{\nabla}_6 \cdot (\psi^{*-} \vec{\nabla}_6 \psi^+ - \psi^+ \vec{\nabla}_6 \psi^{*-}), \end{aligned} \quad (59)$$

where  $\vec{\nabla}_6 = (\vec{\nabla}_{\vec{r}_1}, \vec{\nabla}_{\vec{r}_2})$  is the six-dimensional gradient. From Gauss's theorem, Eq. (59) becomes

$$(E^+ - E^-) \int_{\Gamma_R} \psi^+ \psi^{*-} = -\frac{\hbar^2}{2m} \int_{\Sigma} d\vec{s} \cdot (\psi^{*-} \vec{\nabla}_6 \psi^+ - \psi^+ \vec{\nabla}_6 \psi^{*-}), \quad (60)$$

where  $d\vec{s} = ds \vec{e}_{RL}$ ;  $\vec{e}_{RL}$  is a six-dimensional unit vector orthogonal to, and pointing from the "right"-hand to the "left"-hand side of the hypersurface  $\Sigma$ ,

$$\vec{e}_{RL} = \frac{(\vec{R}_2, \vec{R}_1) - (\vec{R}_1, \vec{R}_2)}{|(\vec{R}_2, \vec{R}_1) - (\vec{R}_1, \vec{R}_2)|} = \frac{1}{\sqrt{2}} (-\vec{\Delta}, \vec{\Delta}), \quad (61)$$

where  $\vec{\Delta} = \vec{R}_1 - \vec{R}_2$ . Expressing  $\psi^\pm$  in terms of the home-base functions,

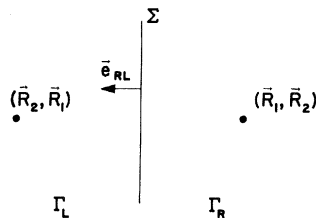


FIG. 11. Geometry of configuration space.

$$\phi_{R(L)} = \frac{1}{\sqrt{2}} (\psi^+ \pm \psi^-)$$

and taking the real part of Eq. (61) one obtains

$$\begin{aligned} (E^+ - E^-) \int_{\Gamma_R} (|\phi_R|^2 - |\phi_L|^2) \\ = -\frac{\hbar^2}{m} \operatorname{Re} \int_{\Sigma} d\vec{s} (\phi_R \vec{\nabla}_6 \phi_L^* - \phi_L^* \vec{\nabla}_6 \phi_R). \end{aligned}$$

The integral on the left-hand side is  $1 + O(J^2)$ , so that to leading order

$$\begin{aligned} J = \frac{1}{2} (E^+ - E^-) &= -\frac{\hbar^2}{2m} \operatorname{Re} \int_{\Sigma} d\vec{s} \cdot (\phi_R \vec{\nabla}_6 \phi_L^* - \phi_L^* \vec{\nabla}_6 \phi_R) \\ &= \frac{\hbar^2}{m} \operatorname{Re} \int_{\Sigma} d\vec{s} \cdot \phi_L^* \vec{\nabla}_6 \phi_R. \end{aligned} \quad (62)$$

This is the surface integral expression we employ. It rigorously gives half the singlet-triplet splitting of  $H(12)$  to leading order, when the "exact" home-base functions are used:

$$\phi_{R(L)} = (\psi^+ \pm \psi^-)/\sqrt{2}. \quad (63)$$

## 2. Relation of the Surface Integral Formula to Perturbation Theory

The theories mentioned at the beginning of this appendix calculate half the singlet-triplet splitting of  $H(12)$  in first-order perturbation theory. We schematically indicate the perturbation expansion for the eigenfunctions  $\psi^\pm$  as follows:

$$\psi^\pm = \psi_0^\pm + \lambda \psi_1^\pm + \lambda^2 \psi_2^\pm + \dots \quad (64)$$

For the "exact" home-base function  $\phi_R$  we thus have

$$\begin{aligned} \phi_R &= (\psi_0^+ + \psi_0^-)/\sqrt{2} + \lambda (\psi_1^+ + \psi_1^-)/\sqrt{2} + \dots \\ &= \phi_R^{(0)} + \lambda \phi_R^{(1)} + \dots \end{aligned} \quad (65)$$

On and near the hypersurface  $\Sigma$  we expect  $\psi^\pm$  and  $\psi_0^\pm$  to be of order  $(J/\epsilon_0)^{1/2} < 10^{-2}$  (here  $\epsilon_0$  is some appropriately defined single-particle energy, e.g.,  $\hbar \Theta_D$ ). We expect the most important corrections  $\lambda^n \psi_n^\pm$  to be of order  $\lambda^n (J/\epsilon_0)^{1/2}$  in this same region. According to Eq. (65) these same estimates apply to the size of  $\phi_R^{(0)}$  and  $\lambda^n \phi_R^{(n)}$  in the neighborhood of  $\Sigma$ . If we were to evaluate Eq. (62) with the approximation  $\phi_R \simeq \phi_R^{(0)}$ , and similarly  $\phi_L \simeq \phi_L^{(0)}$ , we make errors only to order  $\lambda J$ . This is a second-order correction to the singlet-triplet splitting of  $H(12)$ , while the splitting itself is a first-order quantity in perturbation theory. We therefore conclude that *all* first-order contributions to  $J$  which can be obtained using the zeroth-order functions  $\psi_0^\pm$ , are included in the surface integral when the corresponding zeroth-order home-base functions are used, i. e.,  $\phi_R^{(0)} = (\psi_0^+ + \psi_0^-)/\sqrt{2}$ ,  $\phi_L^{(0)} = (\psi_0^+ - \psi_0^-)/\sqrt{2}$ . A crucial factor in this conclusion is that our ex-

pression for  $J$  involves the behavior of the various functions only near  $\Sigma$ . We shall shortly see, in fact, that the cancellation of  $\psi_n^+$  against  $\psi_n^-$  in the "left" space is not very good for the various higher-order terms in Eq. (65). One effect of these terms in Eq. (65) is thus to generate a small "bump" of order  $J/\epsilon_0$  in size in the "left" half-space. While this "bump" might lead to a first-order contribution to a volume integral, it leads to only a second-order contribution in the surface integral. To illustrate this fact, consider the pathological case where  $\phi_R^{(1)}$  in Eq. (65) might actually equal  $\phi_L^{(0)}$ . The arguments we have made above for the surface integral still apply, as  $\lambda\phi_L$  is of order  $\lambda(J/\epsilon_0)^{1/2}$  near  $\Sigma$ .

In order to make further connection with the work of Brandow<sup>15</sup> and others, we write the eigenfunctions of  $H(12)$  as

$$\psi^*(12) = \frac{1}{\sqrt{2}} [\theta_R(12) \pm \theta_L(12)] \Omega^*(12), \quad (66)$$

where  $\theta_R(21) = \theta_L(12)$  and of necessity  $\Omega^*(12) = \Omega^*(21)$ . This is quite rigorous, as given the functions  $\theta_R$  and  $\theta_L$ , we are simply defining the functions  $\Omega^+$  and  $\Omega^-$ . The functions  $\theta_R(12)$  and  $\theta_L(12)$  are chosen to incorporate as much as possible of the localized nature of  $\psi^*(12)$  in the "right" and "left" half-space, respectively. In terms of Eq. (65) the exact home-base function  $\phi_R$  is

$$\begin{aligned} \phi_R &= \frac{1}{2} \theta_R(\Omega^+ + \Omega^-) + \frac{1}{2} \theta_L(\Omega^+ - \Omega^-) \\ &= \theta_R \Omega + \theta_L \Delta \Omega, \end{aligned} \quad (67)$$

where we have defined  $\Omega = \frac{1}{2}(\Omega^+ + \Omega^-)$  and  $\Delta \Omega = \frac{1}{2}(\Omega^+ - \Omega^-)$ . Note that  $\Omega(12)$  and  $\Delta \Omega(12)$  are also symmetric. Similarly

$$\phi_L = \theta_L \Omega + \theta_R \Delta \Omega. \quad (68)$$

The departure of  $\Omega^+$  from  $\Omega^-$  is related to the exchange process (see Guyer and Zane's or Brandow's discussion of the "correlation" term). In the absence of exchange one would have  $\Omega^+ = \Omega^-$ . Thus with exchange  $J$  we expect  $\Omega^+$  and  $\Omega^-$  to differ by terms of order  $J/\epsilon_0$ , i. e.,  $\Delta \Omega$  is of order  $J/\epsilon_0$ . We expect that near the hypersurface  $\Sigma$ , both  $\theta_L$  and  $\theta_R$  are of order  $(J/\epsilon_0)^{1/2}$ ,  $\Delta \Omega$  is of order  $J/\epsilon_0$ , and  $\Omega$  can be of order unity. The arguments of the previous paragraph apply, and so to within errors of  $O(J^2/\epsilon_0)$ :

$$J = (\hbar^2/m) \text{Re} \int_{\Sigma} d\vec{s} \cdot (\theta_L \Omega)^* \vec{\nabla}_{\theta} (\theta_R \Omega). \quad (69)$$

Since  $\vec{e}_{RL} \cdot \vec{\nabla}_{\theta}$  and  $\Omega(12)$  are odd and even, respectively, under permutation of the particles, and  $\theta_L(21) = \theta_R(12)$ , this becomes

$$J = (\hbar^2/m) \text{Re} \int_{\Sigma} d\vec{s} \cdot |\Omega|^2 \theta_L^* \vec{\nabla}_{\theta} \theta_R. \quad (70)$$

What conclusions about the sign and magnitude of  $J$  can be drawn from Eq. (70)? The function

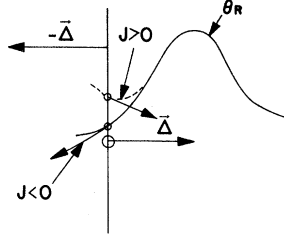


FIG. 12. Sign of  $J$ . The sign of  $J_1$  is determined by the behavior of the relative coordinate wave function in the vicinity of the interface between  $\Gamma_R$  and  $\Gamma_L$ . If the wave function decays as it approaches this interface the sign of  $J$  is negative. If the wave function is increasing as it approaches this interface, the sign of  $J$  is positive. In order for the wave function to be increasing near the interface it must have an extra node (see the dashed line). Since it is not then the ground-state wave function, we argue that  $J < 0$  in the ground state.

$\theta_R(12)$  is localized in the "right" half-space about the point  $(\vec{R}_1, \vec{R}_2)$ , and drops off as one moves away from this point. The quantity  $\vec{e}_{RL} \cdot \vec{\nabla}_{\theta}$  is the derivative in the direction from the point  $(\vec{R}_1, \vec{R}_2)$  towards the point  $(\vec{R}_2, \vec{R}_1)$ , and thus  $\theta_L^*(\vec{e}_{RL} \cdot \vec{\nabla}_{\theta}) \theta_R$  should be negative in the vicinity of the hypersurface  $\Sigma$ . Clearly, if  $\theta_R$  reached some minimum and then began to increase as one approached  $\Sigma$  from the "right"-hand side, the sign of  $\theta_L^*(\vec{e}_{RL} \cdot \vec{\nabla}_{\theta}) \theta_R$  could be positive (see Fig. 12). However, the resultant "bump" that this feature would introduce into the eigenfunctions  $\psi^*$  makes this possibility highly unphysical on the grounds of the cost in kinetic energy. It is therefore evident that the sign of  $J$  determined by Eq. (70) is manifestly negative. This is consistent with the general arguments made elsewhere<sup>10</sup> that the lowest eigenvalue of the Hamiltonian must correspond to a spatially symmetric eigenfunction, and is thus a singlet state for our two-body problem. Further, it is perfectly clear that  $\Omega$ , the short-range correlation function, cannot enter into a discussion of the sign of  $J$ . It can only have an effect on the magnitude of  $J$ , and this effect is discussed at length in the body of this paper. The dominant contribution to the magnitude of  $J$  is due simply to the size and slope of the functions  $\theta_R$  and  $\theta_L$  in the neighborhood of the hypersurface.

Let us repeat our main conclusions and discuss their limitations.

- (1) The sign of  $J$  is negative.
- (2) When the eigenfunctions of the two-body Schrödinger equation are written in the form in Eq. (66) the sign of  $J$  depends in no way upon the short-range correlation function.

(3) Since the surface-integral expression given in Eq. (70) is correct to order  $J^2/\epsilon_0 \approx 10^{-4}J$  it is clear that the surface-integral formula implemented with a given set of approximate home-base functions sums all first-order perturbation-theory contributions calculated with the corresponding approximate eigenfunctions. These conclusions are correct subject to the analytic form chosen for  $\psi^*$  in Eq. (66) and the requirement that  $J$  calculated with a given approximation to the home-base function be reasonably good, i. e.,  $J/\epsilon_0 \ll 1$ .

#### APPENDIX B. COMPUTATIONAL TECHNIQUE

A combined cluster approximation and Monte Carlo technique has been used to evaluate the many-body surface-integral expressions for the (1) and (2) pair- and the (112) triple-exchange frequencies. The former aspect has been discussed in Sec. IV. We describe here the Monte Carlo evaluation of these  $n$ -body cluster integrals. We then describe our tests of this technique. Finally, we point out that this combined approach is far superior to that used previously to calculate the (1) pair-exchange frequency,<sup>17</sup> and that it may also be more generally useful in evaluating other many-body integrals involving wave functions of the form of Eq. (47), i. e., the Jastrow-Gaussian form.

The  $n$ -body cluster integrals discussed in Sec. IV are given by

$$J_P \approx -\frac{\hbar^2 A}{2m} d_p e^{-A d_p^2/4} \times \int d\vec{r}_1 \dots d\vec{r}_n \delta(u_1) \prod_{i=1}^n e^{-A(\vec{r}_i - \vec{R}_i^{av})^2} F_n^2 / \int d\vec{r}_1 \dots d\vec{r}_n \prod_{i=1}^n e^{-A(\vec{r}_i - \vec{R}_i)^2} F_n^2, \quad (71)$$

where

$$F_n(\vec{r}_1, \dots, \vec{r}_n) = \prod_{1 \leq i < j \leq n} f(r_{ij}),$$

and where the permutation  $P$  indicates the exchange process. For the pair frequencies (atoms 1, 2)

$$d_p = \sqrt{2} |\vec{R}_2 - \vec{R}_1| = \sqrt{2} R_{21}, \quad u_1 = \vec{R}_{21} \cdot \vec{r}_2 / d_p, \quad (72)$$

$$\vec{R}_1^{av} = \vec{R}_2^{av} = \frac{1}{2} (\vec{R}_1 + \vec{R}_2), \quad \vec{R}_i^{av} = \vec{R}_i, \quad i \geq 3.$$

For the triple frequencies (atoms 1, 2, 3)

$$d_p = (R_{21}^2 + R_{32}^2 + R_{13}^2)^{1/2},$$

$$u_1 = (\vec{R}_{21} \cdot \vec{r}_1 + \vec{R}_{32} \cdot \vec{r}_2 + \vec{R}_{13} \cdot \vec{r}_3) / d_p, \quad (73)$$

$$\vec{R}_1^{av} = \frac{1}{2} (\vec{R}_1 + \vec{R}_2), \quad \vec{R}_2^{av} = \frac{1}{2} (\vec{R}_2 + \vec{R}_3), \quad \vec{R}_3^{av} = \frac{1}{2} (\vec{R}_3 + \vec{R}_1),$$

$$\vec{R}_i^{av} = \vec{R}_i, \quad i \geq 4.$$

To facilitate a practical Monte Carlo evaluation of these integrals, one must avoid generating the order of magnitude of  $J_p$  in a statistical manner, e. g., a number  $O(10^{-3})$  generated by having non-

negligible contributions to the integral from only one out of every  $10^3$  configurations. This matter is elaborated elsewhere in a treatment of the (1) pair-exchange calculation,<sup>17</sup> where two coordinate transformations were used to put the integral in a form amenable to practical computation. For our present purposes we note that the first transformation used in that work is effectively incorporated in Eq. (71) by our having factored out the Gaussian overlap  $e^{-A d_p^2/4}$ . The second-point transformation used there is necessary for our calculations of the (1) and (2) pair frequencies. Letting  $\vec{r}_i$  and  $\vec{r}_i'$  be the original and transformed coordinate, respectively, it is given by  $\vec{r}_1' = \vec{r}_1 + \frac{1}{2} \rho \hat{r}_{12}$ ,  $\vec{r}_2' = \vec{r}_2 - \frac{1}{2} \rho \hat{r}_{12}$ , and  $\vec{r}_i' = \vec{r}_i$  for  $i \geq 3$ , where  $\rho \lesssim \sigma$  and  $\sigma = 2.556 \text{ \AA}$ . For the pair calculations, then, we use the following form of Eq. (71):

$$J_{\text{pair}} \approx -\frac{\hbar^2 A}{2m} \sqrt{2} R_{21} e^{-A(R_{21}^2 + \rho^2)/2} \times \int d\vec{r}_1 \dots d\vec{r}_n \delta(u_1) \prod_{i=1}^n \exp[-A(\vec{r}_i - \vec{R}_i^{av})^2] V_n / \int d\vec{r}_1 \dots d\vec{r}_n \prod_{i=1}^n e^{-A(\vec{r}_i - \vec{R}_i)^2} F_n^2, \quad (74)$$

where

$$V_n(\vec{r}_1, \dots, \vec{r}_n) = e^{-A \rho r_{12} (1 + \rho/r_{12})} F_n^2(\vec{r}_1', \dots, \vec{r}_n') \quad (75)$$

and

$$u_1 = \hat{R}_{21} \cdot \vec{r}_2 / \sqrt{2}.$$

For calculation of the triple frequency, Eq. (71) is already in adequate form, as the short-range correlations amongst the three atoms have a much less severe effect than in the pair case. In the following, we shall explicitly refer only to Eq. (71). It is to be understood that for the pair frequencies we actually calculate Eq. (74), and so the appropriate  $F_n^2$  should be replaced by  $e^{-A \rho^2/2} V_n$ .

The Monte Carlo evaluations of both numerator and denominator of Eq. (71) were performed simultaneously. For the numerator, it was convenient to work with variables  $u_1, \dots, u_{3n}$  obtained by orthogonal transformation from  $\vec{r}_1, \dots, \vec{r}_n$  in order that the  $\delta$  function could be explicitly integrated (the same transformation defines  $U_i$  in terms of the  $\vec{R}_i^{av}$ ). Separate configurations for the numerator and denominator were generated according to the Gaussian parts of the respective wave functions using the same set of  $3n$  random numbers  $w_i$ ,  $0 \leq w_i \leq 1$ ,

$$u_i = g^{-1}(w_i) / \sqrt{A} + U_i \quad (\text{num}), \quad i \geq 2, \quad (76)$$

$$r_{j\alpha} = g^{-1}(w_i) / \sqrt{A} + R_{j\alpha} \quad (\text{den}), \quad (77)$$

where

$$g(x) = (1/\sqrt{\pi}) \int_{-\infty}^x dt e^{-t^2},$$

$i = 3j - \alpha$ , and  $\alpha = 0, 1, 2$  corresponding to the  $x$ ,



$y$ ,  $z$  directions. The numerator and denominator were obtained [aside from factors of  $(\pi/A)^{(3n-1)/2}$  and  $(\pi/A)^{3n/2}$ ] by averaging  $F_n^2$  over the appropriate sets of configurations. For  $n=8$ , convergence was generally reached between 4000–8000 configurations, and subsequent scatter in the value of  $J_P$  was less than a few percent. For this same value of  $n$ , the running time for 10 000 configurations on the CDC 3800 was about 6 min.

The programs were tested in several ways. The two-body cluster integrals for the (1) and (2) pair frequencies can be reduced to one-dimensional integrals for independent computation. The  $n=2$  Monte Carlo results easily agreed with these independent results to better than 1%. Furthermore, the converged (with  $n$ ) values for the (1) pair frequency agree to within 6% over the whole density range considered with earlier Monte Carlo calculations of this same frequency,<sup>17</sup> which used a considerably different method. This is well within the combined uncertainties of these two calculations. A test of the full many-body nature of the triple-exchange program was made using the test correlation function

$$F_{\text{test}} = \sum_{i < j} e^{-B_{ij}(\vec{r}_{ij} - \vec{R}_{ij})^2},$$

$$B_{ij} = B \quad i, j \text{ near neighbors}$$

$$= 0 \quad \text{otherwise}.$$

While the Monte Carlo calculation with  $F_{\text{test}}$  is of the same order of difficulty as our calculations with the Nosanow correlations, the full integral as well as each of the cluster integrals may be reduced analytically in this case to one-dimensional integrals for independent computation. The independent calculations showed the value of the full integral to be increasingly reduced, and the cluster integral to converge less rapidly, as  $B$  increases. We chose  $B = \frac{1}{32}A$ ,  $A = 1.30 \text{ \AA}^{-2}$  to make the test, in which case the full integral is reduced by more than three orders of magnitude over its value with  $B=0$ , and the  $n=16$  cluster integral is about a factor of 5 larger than the value of the full integral.

The Monte Carlo evaluation of the  $n=16$  cluster integral was found to agree with the corresponding independent calculation to better than 1%.

In a previous calculation<sup>17</sup> of the (1) pair frequency it was seen that the many-body short-range correlation effects in solid <sup>3</sup>He are quite important to the exchange process. That calculation incorporated 54 atoms, with periodic boundary conditions, in the usual attempt to mimic an infinite lattice. The results reported in Sec. IV of this paper, however, show that those many-body effects which are most important to the exchange process are associated almost entirely with only those few immediately surrounding neighboring atoms which in some sense directly get in the way of the exchanging atoms. This fact permits a distinct improvement in the speed and accuracy of the Monte Carlo calculations in that one need only evaluate relatively low-dimensional integrals. (The present method is about an order of magnitude faster than the earlier one.) A second improvement exhibited in our present technique is that rather than the full wave function, only the Gaussian part is used to generate the configurations. This allows one to handle the  $\delta$  function in a simple and rigorous manner. The  $\delta$  function was a source of some difficulty in the earlier work.

We feel that the combined cluster approximation and Monte Carlo technique used here may be useful in evaluating other many-body integrals involving Jastrow-Gaussian wave functions. In addition to exchange integrals, single-particle densities and matrix elements of two-body potentials should be amenable to this technique. We have in fact used it successfully<sup>33</sup> in calculating the single-particle density for bcc <sup>4</sup>He. Recent criticism of cluster approximations<sup>34</sup> is really directed at the two-body approximations most often used. We suggest that retention of a more realistic number of neighboring atoms in the cluster approximations will yield quite good approximations, and that such relatively low-dimensional integrals may be evaluated fairly quickly and accurately by the Monte Carlo technique.

\*Work supported in part by the National Science Foundation and the Alfred P. Sloan Foundation.

<sup>1</sup>Present address: Department of Physics, Cornell University, Ithaca, N. Y. 14850.

<sup>2</sup>R. A. Guyer, in *Solid State Physics*, edited by F. Seitz and D. Turnbull (Academic, New York, 1969), Vol. 23.

<sup>3</sup>R. A. Guyer, R. C. Richardson, and L. I. Zane, *Rev. Mod. Phys.* **43**, 532 (1971).

<sup>4</sup>J. H. Hetherington, *Phys. Rev.* **176**, 231 (1968).

<sup>5</sup>A. F. Andreev and L. M. Lifshitz, *Zh. Eksp. Teor. Fiz.* **56**, 2057 (1969) [*Sov. Phys.-JETP* **29**, 1107 (1969)].

<sup>6</sup>R. A. Guyer and L. I. Zane, *Phys. Rev. Lett.* **24**, 660 (1970).

<sup>7</sup>M. F. Panczyk and E. D. Adams, *Phys. Rev.* **187**, 321 (1969).

<sup>8</sup>E. D. Adams, W. Kirk, and S. B. Trickey, *Rev. Mod. Phys.* **44**, 668 (1972).

<sup>9</sup>R. C. Richardson, E. R. Hunt, and H. Meyer, *Phys. Rev.* **138**, A1326 (1965).

<sup>10</sup>L. H. Nosanow and W. J. Mullin, *Phys. Rev. Lett.* **14**, 133 (1965).

<sup>11</sup>D. Thouless, *Proc. Phys. Soc. Lond.* **86**, 893 (1965).

<sup>12</sup>J. H. Hetherington, W. J. Mullin, and L. H. Nosanow, *Phys. Rev.* **154**, 175 (1967).

<sup>13</sup>L. H. Nosanow and C. M. Varma, *Phys. Rev.* **187**, 660 (1969).

<sup>14</sup>R. A. Guyer and L. I. Zane, *Phys. Rev.* **188**, 445 (1969).

<sup>15</sup>C. Ebner and C. C. Sung, *Phys. Rev. A* **4**, 1099 (1971).

<sup>16</sup>B. H. Brandow, *Phys. Rev. A* **4**, 422 (1971); *Ann. Phys.* **74**, 112 (1972).

- <sup>16</sup>E. Ostgaard, *J. Low Temp. Phys.* **1**, 471 (1972).  
<sup>17</sup>A. K. McMahan, *J. Low Temp. Phys.* **8**, 115 (1972); *J. Low Temp. Phys.* **8**, 159 (1972).  
<sup>18</sup>W. P. Kirk and E. D. Adams, *Phys. Rev. Lett.* **27**, 392 (1971).  
<sup>19</sup>L. I. Zane, *Phys. Rev. Lett.* **28**, 420 (1972); *J. Low Temp. Phys.* **9**, 219 (1972); and *Phys. Lett. A* **41**, 421 (1972).  
<sup>20</sup>C. Herring, in *Magnetism*, edited by G. Rado and H. Suhl (Academic, New York, 1968), Vol. II B.  
<sup>21</sup>L. H. Nosanow, *Phys. Rev.* **146**, 120 (1966).  
<sup>22</sup>L. H. Nosanow, Quantum Crystals Conference, Banff, Canada (1971) (unpublished).  
<sup>23</sup>R. T. Johnson, R. F. Rapp, and J. C. Wheatley, *J. Low Temp. Phys.* **6**, 445 (1972).  
<sup>24</sup>W. P. Kirk, E. B. Osgood, and M. C. Garber, *Phys. Rev. Lett.* **23**, 833 (1969).  
<sup>25</sup>J. Sites, D. Osheroff, R. C. Richardson, and D. M. Lee, *Phys. Rev. Lett.* **23**, 835 (1969).  
<sup>26</sup>P. A. M. Dirac, *Proc. R. Soc. A* **123**, 714 (1929).  
<sup>27</sup>W. Heisenberg, *Z. Phys.* **49**, 619 (1928).  
<sup>28</sup>J. H. Van Vleck, *Theory of Electric and Magnetic Susceptibilities* (Oxford U.P., London, 1932).  
<sup>29</sup>H. Meyer, *J. Appl. Phys.* **39**, 390 (1968); and Ref. 2.  
<sup>30</sup>See Ref. 20, pp. 125–160, and references therein.  
<sup>31</sup>J. P. Hansen and D. Levesque, *Phys. Rev.* **165**, 293 (1968).  
<sup>32</sup>D. Osheroff, R. C. Richardson, and D. M. Lee, *Phys. Rev. Lett.* **28**, 885 (1972).  
<sup>33</sup>A. K. McMahan and R. A. Guyer, in Proceedings of the Thirtieth International Conference on Low Temperature Physics (to be published, 1972).  
<sup>34</sup>N. R. Werthamer, Conference Summary, Banff Conference on Quantum Crystals, 1971 (unpublished).

## Sound-Modulated Flow of Superfluid Helium through a Small Orifice: An Attempt to Observe the ac Josephson Effect\*

P. Leiderer and F. Pobell†

*Physik-Department, Technische Universität, München, Germany*

(Received 2 October 1972)

Two chambers filled with superfluid helium to different levels were connected by a small orifice (10–15  $\mu\text{m}$ ). The flow of the liquid through the orifice was modulated by a sound field. With one experimental apparatus only a continuous flow was observed. With a modified apparatus it was possible to obtain stable states with no net flow at finite level differences between the baths. The spacing between these states is inversely proportional to the sound frequency. It depends on the total height of the liquid in one of the baths and not on the level difference between them. We conclude that the stable states of zero flow result from ultrasonic standing waves of the superfluid in one of the chambers. A phase coupling or Josephson effect can be excluded as an explanation for these states.

### I. INTRODUCTION

One of the most fascinating aspects about superfluid helium is the similarity of many of its properties to the properties of metallic superconductors. The many analogies between these superfluids suggest the possibility of observing the ac Josephson effect in He II. Experiments whose results were interpreted as the ac Josephson effect in superfluid helium were reported some years ago in Refs. 1 and 2, and recently in Ref. 3. In these experiments two chambers filled with superfluid helium to different levels were connected by a small orifice, as shown in Fig. 1. Although this orifice is very large (about 10  $\mu\text{m}$ ) compared to the coherence length of He II it is supposed to act as a "weak link" between the two baths. Below the orifice an ultrasonic transducer is mounted. Its sound field can modulate the flow of superfluid through the orifice. The authors<sup>1–3</sup> observed interruption of flow at distinct level differences  $\Delta z$  between the two baths. The arrests seem to occur whenever

$$n_1 m g \Delta z = n_2 h \nu, \quad (1)$$

where  $n_1$  and  $n_2$  are integers,  $m$  the mass of a  $^4\text{He}$

atom,  $g$  the gravitational acceleration,  $\Delta z$  the level difference,  $h$  Planck's constant, and  $\nu$  the frequency of sound.

This Josephson frequency relation proposed by Anderson<sup>4</sup> is based on two concepts: (i) There is a phase slippage of the superfluid order parameters of the two coupled baths due to a chemical potential difference between them. This difference results from the difference  $m g \Delta z$  in gravitational potential. (ii) The variation of the phase may be synchronized by an external sound field of frequency  $\nu$ . Then the net flow between the two baths may be interrupted whenever the difference in gravitational potential is compensated by a constant phase slippage. This phase slippage could result from the generation and motion of vortices in the orifice at a rate  $(n_2/n_1)\nu$ . Details can be found in Refs. 1–4. Several aspects of these experiments have remained unexplained, particularly with regard to what is happening at the orifice. In addition, steps in the flow curve have only been observed when the difference in the chemical potential was created by a gravitational head difference.<sup>5</sup>

In 1968 we tried to repeat and possibly extend the above-mentioned experiments by varying some ex-